
Study of Inter-annual Variability of Chlorophyll in the Red Sea

Abubakr Elsayed Salman Elawad



Thesis for the degree of Master of Science (MSc)

UNIVERSITY OF BERGEN

Geophysical Institute

October 2012

To my family and close friends :)

Acknowledgements

At the beginning, I find my self not familiar with many aspect of this work and I had to seek help. This help enabled me to overcome different obstacles and difficulties and made it possible for me to complete my work successfully. I am really grateful and thankful to the people who took the time and effort to guide me through different parts of this project.

First of all, I would like to give many thanks to my supervisors:

Dr.*Anton Korosov*, you taught me all of the softwares which I used on this work, and you were patient when you were teaching them to me, and also thank you for the comments you sent me during my work in Sudan. It never felt as though you were that far away..

Dr.*Abdirahman omar*, thank you so much for your supervision, you always kept your door open whenever I needed you.

Dr.*IngunnSkjelvan*, you clarified things to be understandable.

I would like to give special thanks to the geophysical institute represented in Dr. *Knut Barthel*, the leader of this program. You were our father, I will never forget all the moments you helped us. You kept your smile even with the all troubles you solved. thank you so much .

Thanks to the institute of marine research IMR researchers and staff in *Sudan* for their support. specially *Salma* and *Waleed*.

I would like to give special thanks to Dr.*Mohammed Alfaki* and his family, he was like our elder brother here I Norway, whenever I needed him, I found him. . . thank you so much Mohammed.

Many thanks to all the Sudanese students I met in Fantoft during my stay. I got many helps from them. *Mohammad Madani*, *Alfatih Ali*, thank you so much.

I would like to thank Dr.*Mohamed Babekir* from NERSC, I got alot of advices from him.

I would like to thanks my best friends In Norway, *Alexander Sløk Mjelde* and *Tina Montgomery* for the all help I have get from them . thank you som much.

Acknowledgements

Thank you *my colleagues* for the nice moments we have had together during these two years.

Finally, thank you so much to my *family* in Sudan for every thing

Study of Inter-annual Variability of Chlorophyll in the Red Sea

Thesis for the degree of Master of Science (MSc)

Abstract

This thesis studies and estimates interannual chlorophyll-a concentration in the Red Sea water using SeaWiFS, MERIS and MOIDS data. We use the data of Chlorophyll-a (CHL-a) for the period from 1998 to 2009 as well as other physical parameters such as, sea surface temperature (SST), photosynthetic available radiation (PAR), wind and mixed layer depth (MLD) to study what control the interannual variations of phytoplankton blooms in the Red Sea. The area under study is divided into three zones which cover the north, the middle and the south zones of the Red Sea.

When considering the data seasonally, the CHL-a shows that blooms always occur in the Red Sea during winter. For each zone, the start and the end of the blooms are different from other zones. During all three zones, the CHL-a is increasing during winter and decreasing during the summer for example, the average high value of CHL-a in the north zone during the blooms is (0.26 mg/m^3) and the minimum value is (0.14 mg/m^3).

only in the south the blooms started in the summer in September and the highest value of CHL-a during the blooms recored is the south too (0.9 mg/m^3).

The study shows that the physical parameters have effect in the blooms sizes In each zone, significant correlations between CHL-a and some of the physical parameters is found indicating how physical processes may control the phytoplankton blooms in the study area. such as the wind in the south showed up the controloing of CHL-a by the positive correlation that CHL-a and wind had during the blooms (0.740).

Interannual variations are computed as monthly anomalies relative to the 1998-2009 monthly climatology. In this way, the effect of co-variation between different variables on the seasonal time scale is minimized, The anomaly data showed clear

Abstract

interannual variations in almost all parameter and zones. Strong co-variations between CHL-a and the physical parameters showed that physical process have effect on the interannual changes in the phytoplankton blooms in the Red Sea.

Few highly anomalous years in some of the parameters produce a weak long-term (1998-2009) trends. Such as, in the southern zone of the Red Sea when the value of $R^2=0.0157$ according the high value of CHL-a in 2008 and 2009 approximately 0.28 mg/m^3 for both of them. The value of R^2 becomes 0.0009 when these two years have been removed.

October 2012 – Bergen, Norway,
Abubakr Elsayed Salman Elawad

Contents

Abstract	vii
1 Aims and motivations	1
2 Literature review	3
2.1 Phytoplankton	3
2.1.1 Phytoplankton and chlorophyll	3
2.1.2 Factors limiting the growth of phtoplankton	4
2.1.3 Methodes of chlorophyll determination	5
2.1.4 Previous studies	6
2.2 Remote sensing technique	6
2.2.1 Examples of Ocean Colour Satellite sensors	7
2.2.2 Case-1 and case-2 water	8
2.3 Area of study	8
2.3.1 The Red Sea	8
2.3.2 The Red Sea circulation and water mass	10
2.3.3 The Red Sea salinity and surface Temperature	12
2.3.4 The Red Sea nutrients and early studies	13
3 Data sources and Data processing	15
3.1 Data sources	15
3.1.1 Download of data with WGET	15
3.2 Data processing	17
3.2.1 Operations in BEAM/VISAT	17
3.2.2 Operations on Excel	20

4	Results and discussion	23
4.1	the North zone	23
4.1.1	Physical parameters and their effects on the CHL-a	25
4.2	the Middle Zone	31
4.3	the South zone	37
5	Conclusion and Recommendation	43
	Bibliography	45

List of figures

2.1	The map shows the bathymetry and the location of the Red Sea, the thin arrows indicate to wind direction during summer, while the thick arrows indicate the wind directions in winter (Ali, 2008).	9
2.2	Mean surface circulation from MICOM simulation. At the left hand, wind during winter. The right hand figure illustrates summer circulation (Sofianos and Johns, 2002).	10
2.3	Sketch Illustrates the winter and summer water exchange in the south of the Rd Sea, RSW and RSDW are the Red Sea Water and Red Sea Deep water, the Red Sea inflow water is both RSW and RSDW, GDSW and GAIW are Gulf of Aden surface and intermediate water, respectively (Smeed, 1997).	11
2.4	Annul mean of sea surface temperature (a), and Annual mean of Salinity (b) to the Red Sea from MICOM simulation (experiment E1, average over the last 9 years of simulation (Sofianos and Johns, 2003).	12
3.1	Beam/ ViSAT software, the program which is used to analyse the satellite data.	18
3.2	the zoomed map of the Red Sea. The SST picture shows the map of the Red Sea on BEAM/VISAT.	19
3.3	Map shows the distributions of the pins in the three zones of the Red Sea, for each zone, 50 pins were distributed carefully to cover the whole zone.	20
3.4	Illustrates the SST quality control, the columns are the weekly SST data while the yellow and green rows are the mean and STDEV, respectively.	21
3.5	the smoothed data (monthly mean) for CHL-a and other physical parameters. MLD data started from 2003.	22

List of figures

4.1	Illustrates the CHL-a pictures in different seasons in 2001. A and B pictures during winter. A in January and B picture in December. While the C and D during the summer. C in June and D in April. The pictures show that the blooms were in winter.	23
4.2	weekly concentration of surface Chlorophyll-a (mg/m^3) from the period 1998 until 2009 in the north zone of the	24
4.3	Monthly mean concentration of CHL-a mg/m^3 to the all years from year 1998 until 2009 in the north zone of the Red Sea.	26
4.4	Monthly mean of the Sea Surface temperature for the year from 1998 until 2009 in the north zone of the Red Sea.	27
4.5	Monthly mean of Photosynthetically available radiation, from the period 1998 until 2008 to the north zone of the Red Sea.	27
4.6	Monthly mean of mixed layer (m)depth from the period 2003 until 2007, north zone of the Red Sea. The figure shows unclear date specially 2005 and 2006.	28
4.7	Monthly data of wind (m/s) for the period from the period 1998 to 2009.North zone of the Red Sea.	28
4.8	Monthly anomalies plot of CHL-a with the physical parameters in the north zone of the Red Sea, the different between each month and the month climatology	29
4.9	Monthly concentration of chlorophyll-a from the period 1998 to 2009 in the Middle zone of the Red Sea.	32
4.10	Monthly mean of Sea Surface temperature (SST) for the period from 1998 to 2009 in the Middle zone of the Red Sea.	33
4.11	Monthly data of Photo synthetically available radiation (PAR) for the period from 1998 until 2009 in the Middle zone of the Red.	33
4.12	Monthly data of mixed layer depth (MLD) for the Period from 1998 until 2009 in the Middle zone of the Rea.	34
4.13	Monthly data of wind speed from the period 1998 until 2009 in the middle zone of the Red Sea.	34
4.14	Monthl anomalies of chlorophyll-a with other physical parameters during winter months, the plot for the middle zone of the Red Sea.	35

4.15	picture of january-8 during blooms for the Red Sea and North zone of the Arabian Sea. Showing the high blooms in north of Arabian Sea and south of the Red Sea	37
4.16	Monthly concentration of chlorophyll-a to the period from 1998 until 2009. South of the Red Sea	38
4.17	Monthly data of sea surface temperature SST, to the south zone of the Red Sea from the period 1998 until 2009.	39
4.18	Monthly data of photosynthetic available radiation PAR to the south zone of the Red Sea from the period 1998 until 2009.	39
4.19	Monthly data of mixed layer depth (MLD) for the years from 2003 until 2007 to the South zone of the Red Sea. The monthly south look smooth as the middle	40
4.20	Monthly data of WIND for the period from 1998 until 2009 in the Middle zone of the Red Sea.	40
4.21	plot of Anomalies of CHL-a with other parameters in South zone of Red Sea. For each parameter, each monthly value was subtracted from monthly climatology	41

List of tables

3.1	Satellites and model data with their units, sources, covering areas, frequency. CHL-a is chlorophyll-a, SST is sea surface temperature, PAR is photosynthetic available radiation and MLD is mixed layer depth. While S.R and T.R are spatial resolution and temporal resolution, respectively.	16
4.1	Monthly Correlation of CHL-a with other physical parameters (SST, PAR, wind and MLD) north zone of the Red Sea.	29
4.2	The anomalies correlations of CHL-a with other parameters in north zone of the Red Sea. The table contains values PAR and SST shows high values of correlation.	30
4.3	Monthly correlation of CHL-a with the physical parameters in Middle Zone of the Red Sea. SST is sea surface temperature, PAR is photosynthetic available radiation and MLD is mixed layer depth.	35
4.4	Anomalies correlation of CHL with other physical parameters in Middle Zone of the Red Sea	36
4.5	Monthly correlations of CHL with other parameters South Zone of the Red Sea.	41
4.6	Anomalies correlation of CHL with other parameters South Zone of Red Sea	41

Chapter 1

Aims and motivations

The aim of this thesis is to study the inter-annual variability of chlorophyll-a in the Red Sea, which is one of the least investigated seas in the world. In addition to that, we want to find out which physical parameters (for example, sea surface temperature, photosynthetically available radiation, mixed layer depth and wind) have effect in controlling CHL-a bloom.

The motivations to do this work are

- There were many studies that took place in the world's oceans to investigate the chlorophyll and its dynamic. Only a few of them were found in the Red Sea and this is because of data limitation as result of political barriers and the nature of the Red Sea which was unknown yet.
- In the past, scientists used ships and boats to collect the samples. With the advance of the technology such as the satellites, one can easily study the whole Red Sea area or even focus on some areas.
- Many satellites data are free, so it will encourage scientists to do more research which cannot be done if the data are expensive.

The reasons behind the selection of these three zones in the Red Sea are as follows: Each zone is different from the other in terms of depth and the monsoon, in addition to the connections of these zones with the open oceans.

The reasons of using these parameters data are: The photosynthesis process is a chemical reaction and it needs nutrients, light and carbon dioxide as the main factors. Data of photosynthetic available radiation (PAR) is used to determine how much light is incident to the water. The increase of temperature accelerates the reaction rate and that is Sea surface temperature data is used here. The mixed layer depth

Section 1.0.

brings nutrients from the bottom to the upper water layers and these nutrients are important to the photosynthesis process. The wind pushes the rich water of nutrients to the area which has low nutrients.

Environmentally, we all know the increase of greenhouse gas CO₂ leads to global warming, this study will help to predict the share of the Red Sea to decrease global warming, which is one of the main factors of increasing the temperature of the Earth.

Chapter 2

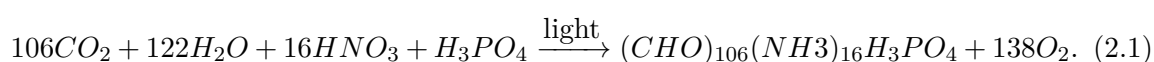
Literature review

2.1 Phytoplankton

2.1.1 Phytoplankton and chlorophyll

The name of phytoplankton came from the Greek *phyton* which means plant, and the *planktos* which means wandering or movements (Jeffrey et al., 1997). The photosynthesis process as in Equation (2.1) is used by phytoplankton to fix the inorganic carbon to carbohydrate, the opposite process is called respiration or remineralisation which is the break down of the organic matter to inorganic forms (see Equation (2.2)).

Photosynthesis



Remineralization/respiration



Phytoplankton plays an important role for showing the colour of the oceans water, it contains the chlorophyll which absorbs the sun light in the green and red bands and makes backscattering from deep blue to green, and the colour depends on the phytoplankton concentration (Yentsch, 1960).

According to [Jeffrey et al. \(1997\)](#) phytoplankton play an important role in the oceans, in the biological sense as it is the first marine food which is grazed by oceanic animals called zooplankton, the food chain expands until it reaches the fish and other marine mammals. The second role is phytoplankton which contribute to the global carbon cycle by fixing carbon dioxide gas to carbohydrates and that will help when considering about the global warming and environmental concepts.

2.1.2 Factors limiting the growth of phytoplankton

The amount of phytoplankton productivity is controlled by the limitation of concentration of some elements which are (N, Fe, Si, and P) which are important for photosynthesis ([Chisholm and Morel, 1991](#)), and sometimes light limitation which occurs during the vertical mixing ([Siegel et al., 2002](#)). Other study was investigated by [Eppley et al. \(1973\)](#) stated that the elements P and N are the limited factors which control the phytoplankton blooms. In addition to the factors in the water itself, there are many external factors control the phytoplankton bloom.

2.1.2.1 Sea Surface Temperature(SST) and algorithm

Half of solar radiation that incidents on the earth is absorbed from the total amount of radiation by the ocean surface, about ($175 \text{ Einstein/m}^2/\text{day}$) of it creates warming ([Gill, 1982](#)). During the day, the surface of an ocean reaches a temperature equal to the losses from the incoming radiation (solar radiation). The flux of water is produced as evaporation during the process is determined by sea surface temperature (SST). As [Minnett et al. \(2011\)](#) states the skin SST is a few mms deep and it measures by infrared radiometers. Bulk SST can be measured by using thermometers which are meters deep in water.

To measure sea surface temperature, there are number of algorithms that can be used. The main idea here is to measure the skin temperature which is a few mms in water. The calculation depends on the emissivity of the radiation which is leaving the water surface. Since there are some overlaps between the radiations from the water surface and the radiations from the clouds and aerosols, the algorithm aims to correct this overlapping by adding some coefficients to the algorithm equation, for more details see ([Robinson, 2010](#)).

2.1.2.2 Photosynthetic available radiation (PAR)

The photosynthesis available radiation is defined as a quantum energy expressed in Einstein/m²/day between the range of 400-700nm of spectra flux from the sun (Frouin et al., 2001). Both the physical and biological processes can be affected by incoming solar radiation. Physically the solar radiation responsible for an oceanic circulation due to the heat transport, while the biologicals will be affected by photosynthesis process, where solar radiation is a main factor (Frouin et al., 1989). According to Barker (1935), light is a limiting factor in the photosynthesis process in ocean. Light intensity is a major factor in the photosynthetic rate.

2.1.2.3 Mixed layer depth

Mixed layer depth depends on other parameters, and the study of mixed layer depth connects with the study of different parameters which control it, these parameters are; temperature, salinity and density. MLD and sea surface temperature are related to each other, thickness of MLD relates to heating (SST) (de Boyer Montégut et al., 2004). To connect mixed layer depth with biological activities, in euphotic zone, the mixed layer can be seen as an important factor during these processes (Morel and André, 1991). Half of the water in the oceans are tropical and subtropical (Mann and Lazier, 2006). The tropical profile of mixed layer shows that there is a boundary between mixed layer and cooler water by sharp pycnocline. The study of mixed layer concept is useful to determine the nutrients and iron cycling in the surface which is important for photosynthesis processes.

2.1.3 Methodes of chlorophyll determination

The methods are used to measure the chlorophyll algae are more, one of them is called the batch technique. It depends on taking samples and doing many processes such as filtering. For more see (Nielsen, 1978). There are some experiments used for measuring such as ¹⁴C fixation. These kind of experiments are expensive and need more time. Therefore, the *Remote Sensing* technique is used instead according to many good properties which the remote sensing technique has, see more in Section 2.2.

2.1.4 Previous studies

There are more studies mentioned the phytoplankton blooms and what the main factors controlling the bloom. One of the studies was in along the southern coasts of Java and Sumatra by [Susanto and Marra \(2005\)](#) who investigated that the high concentration of chlorophyll-a according to the southeast monsoon which was the major factor controlling of the timing and quantity of the chlorophyll-a bloom.

Some study has done in the Arabian Sea, shows interannual variability of CHL-a in the Sea and Its Gulfs by [Sarma \(2012\)](#) who investigated that the chlorophyll-a blooms during the Southwest and Northeast monsoons and with this monsoon, the increase of the mean chlorophyll-a seasonally during the 1998 and 2004 increased the trend in the Southwest of the Arabian Sea.

2.2 Remote sensing technique

The story of remote sensing started in 1858 when the first aerial photographs were taken from Balloon near Paris ([Butler, 1988](#)). Fifty years later, a camera was used to do this mission on film emulsions and a photograph was taken from a platform. The first photograph which was taken from an airplane was in Italy in 1909 by Wilbur Wright. Most of the photographs which were taken were oblique because the balloons and airplanes were not high enough to take vertical shots until the 1930s when standard aerial photography became the standard information source.

Most photographs were taken of the military regions because of the war at that time. Later, the remote sensing technique was used to achieve many works and especially so in the ocean where it is not easy to reach those places to take samples.

We all use our senses to be in touch with what we deal with every day, by hearing, smelling or seeing. This means that we deal with things that are close to us, nevertheless when we use a word (remote), it seems something has a distance from us to touch. Remote sensing is defined as the study of things from a distance ([Brock and McClain, 1992](#)), or the study of places, lands or oceans by using electromagnetic radiation properties without being able to touch the data called remote sensing ([Martin, 2004](#)).

2.2.1 Examples of Ocean Colour Satellite sensors

Ocean colour satellites came to the existence earlier when Coastal Zone Colour Scanner (CZCS) was launched in 1978 by NASA. The mission of CZCS is to observe the biological oceanography (Aiken et al., 1992). It was working on four bands in the visible in wavelengths 443, 520, 550 and 670nm, and one band in near infrared (NIR) at 750nm. To measure SST it had thermal infrared band (10.5 to 12.5 μm) (Hovis et al., 1980). In 1986 the CZCS stopped working because of a problem in the sensor (Evans and Gordon, 1994). Later in 1997, SeaWiFS was launched to follow CZCS but with extra bands to provide full and more accurate data (Hooker et al., 1992). The name of SeaWiFS is an abbreviation of the full name Sea-viewing Wide Field of view Sensor. It has swath width of 2800km with scan angle range of -58.3° to $+58.3^\circ$. SeaWiFS came into existence mainly to give a quantitative bio-optical data to the all global oceans within 48 hours (NASA, 2012b). MODIS is used for both visible and infrared. The abbreviation stands for Moderate Resolution Imaging Spectroradiometer and this instrument is carried on the AQUA and TERRA satellites, the scan width is 2300km with a range angle between $(+5$ and $-5)$, it has 36 bands and with $(0.4-14.4\mu\text{m})$ as spectral range. MODIS gives global coverage every 1-2 days (Martin, 2004). AQUA and TERRA orbits are different from each other in a time and location that the instruments crossing the all glob. TERRA is crossing the equator in the morning from north to south. In AQUA, it is during afternoon crossing and the direction is from south to north (NASA, 2012a).

The European Medium Resolution Imaging Spectrometer (MERIS) was launched on ENVISAT in March 2002 and it has a global coverage of three days with spatial resolution of 300m and 1200m with full and reduced resolution, respectively through 15 bands in visible and infrared (Kneubuehler et al., 2003).

Since the ocean colour satellites came into an existence, they have always needed more complex formulas to calculate algorithms, the first algorithm to calculate the chlorophyll concentration. The scattered light from phytoplankton pigments is detected by the satellite sensor. In a phytoplankton's pigments, the scattered colour is green, the more green colour, the more pigments produced by phytoplankton (Robinson, 2010). So the algorithm to calculate the phytoplankton biomass according to the (Equation (2.3)) is a simple equation to calculate chlorophyll concentration and

therefore the complex equations came later into use but still they depend on this simple equation.

$$C = A \left(\frac{R_{550}}{R_{490}} \right)^B \quad (2.3)$$

While C is chlorophyll concentration, R_λ is the reflectance radiance toward the sensor, A and B are empirically derived coefficients, they are used for many open-ocean situations, that why the algorithm can be widely useful. For more details see ([Martin, 2004](#)).

2.2.2 Case-1 and case-2 water

In ocean color classification, there are two water cases, case-1 and case-2 water. When the interaction between incident light by phytoplankton is higher than other suspended materials, that is then called case-1. Where chlorophyll and carotenoids are important in the absorption. In case-2 water, inorganic materials play an important role in the absorption of the incident light ([Moore et al., 2001](#)). In all two cases, yellow dissolved substances are observed. In the world's water oceans, the ratio between Case-1 and case-2 is about 9:1 ([Sathyendranath et al., 2000](#)). We find case-2 water in rivers runoff in coastal regions.

2.3 Area of study

2.3.1 The Red Sea

The Red Sea is a narrow basin of water located between (12:5°N) and (30°N) with a total area of approximately 4.51×10^5 km². The maximum depth in this sea is more than 2500m ([Smeed, 2004](#)).

The Red Sea connects the Arabian Sea and Mediterranean Sea through two canals, the Suez Canal in the north and Bab el mandeb from the south. There is no river inflow to the Red Sea and high solar energy is always there according to tropical location. Net evaporation losses in the Sea are more than (210cm/yr) ([Shaikh et al., 1986](#)).

The Red Sea stretches from north-west to south-east. Prevailing Winds in summer are from the North-East, in winter- from the south-west. These two winds control

the Red Sea's water movement (Patzert, 1974). The movements of water according to the north-west monsoon in summer, pushes The Red Sea water to the south with a velocity which is 15-20 cm/s. In winter the water reserves as a result of inflow of water (Wikipedia, 2012).

Additionally, there are other studies, such as the one by Patzert (1974) which divided the Red Sea to two sections, north of (19°N) this only by the Wind from north-northwest occurs during the whole year, south of (19°N) is controlled by two monsoons during the year, south-southwest during the winter and north-northwest during summer see Figure 2.1.

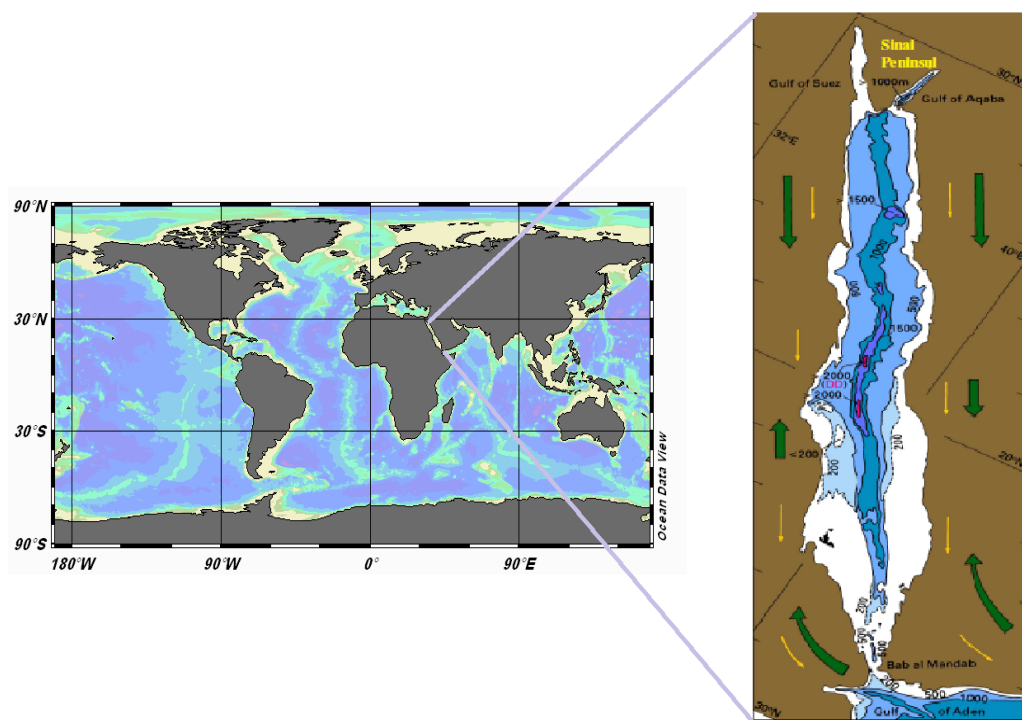


Figure 2.1: The map shows the bathymetry and the location of the Red Sea, the thin arrows indicate to wind direction during summer, while the thick arrows indicate the wind directions in winter (Ali, 2008).

2.3.2 The Red Sea circulation and water mass

In general, the world's ocean water circulation is due to the wind and thermocline. Because of the two monsoons that blow through the years in the Red Sea, the two sites which face the wind have special circulation during the two seasons. The south part of the Red Sea is strongly affected by this circulation throughout the year. As Miami Isopycnic Coordination Ocean (MICOM) simulation (Sofianos and Johns, 2002), illustrates that the south of the Red Sea surface water has cyclonic and anticyclonic rotation during summer and winter, respectively, as result of the two monsoons which take place in the Red Sea. According to the strong SW wind in winter, the high exchange in Bab el Mandeb strait with maximum velocity of more than 20cm/s, and that does not happen in summer, this is described in (Figure 2.2). In the north, especially at 25°N, the strong cyclonic gyre takes place with maximum velocity of 40cm/s (Sofianos and Johns, 2002).

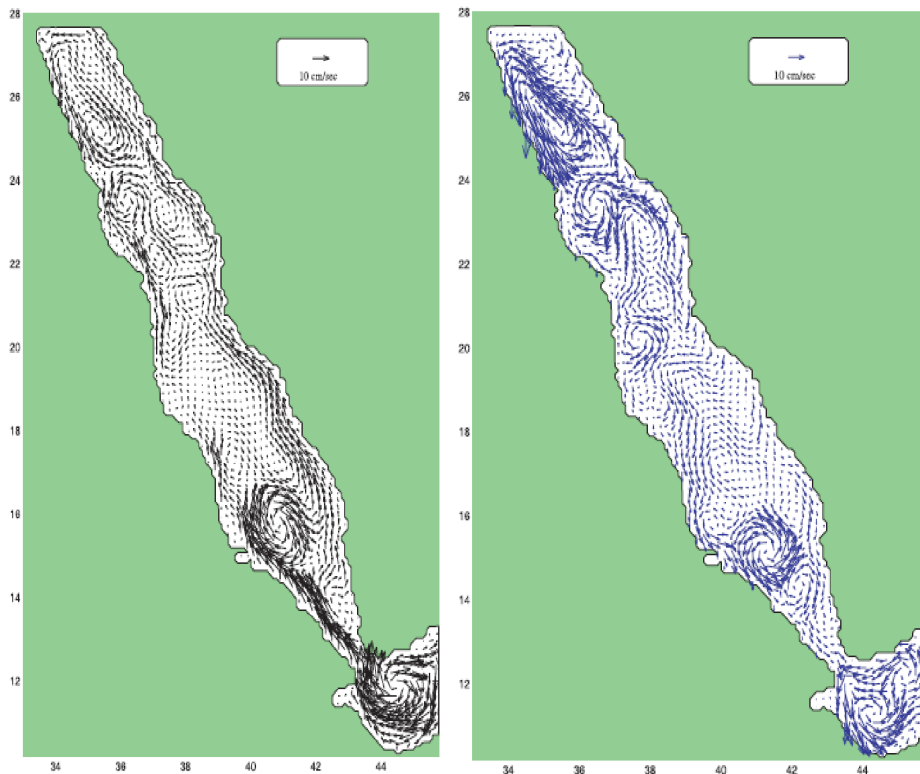


Figure 2.2: Mean surface circulation from MICOM simulation. At the left hand, wind during winter. The right hand figure illustrates summer circulation (Sofianos and Johns, 2002).

The main reasons of forming the Red Sea water is the inflow and outflow water during Bab el Mandeb in the south. That because of the north part has less contribution through the Suez canal. At each depth, the waters of the Red Sea formed in a different way than the other depth. For instance, during the winter, the deep Red Sea water (RSDW) is formed when the water from the north becomes denser as result of the evaporation. After this saline and dense water sinks, the Red Sea deep water (RSDW) is formed. The Red Sea water (RSW) and RSDW flow out through Bab Elman dab all year round (Pratt et al., 1999, 2000). in winter and with the south west monsoon, the RSW and RSDW which they lose through Bab el mandeb strait compensated by the Gulf of Aden surface water(GASW) which has inflow to the Red Sea during winter. Gulf of Aden intermediate water (GAIW) occurs as result of upwelling during south-west monsoon from June to October (Smeed, 1997, 2000; Sofianos and Johns, 2002), this water move into the Red Sea to become more than the outflow of RSDW and RSW that is described in Figure 2.3.

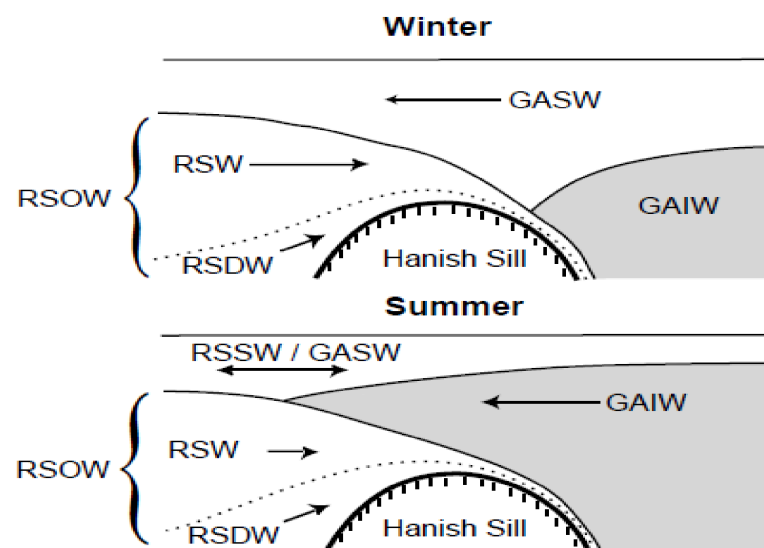


Figure 2.3: Sketch Illustrates the winter and summer water exchange in the south of the Rd Sea, RSW and RSDW are the Red Sea Water and Red Sea Deep water, the Red Sea inflow water is both RSW and RSDW, GDSW and GAIW are Gulf of Aden surface and intermediate water, respectively (Smeed, 1997).

2.3.3 The Red Sea salinity and surface Temperature

According to the MICOM (Miami Isopycnic Coordinate Ocean Model), the annual mean of sea surface temperature in the Red Sea is in the range of (24°C–30°C) in the north of the Red Sea. While the annual mean of salinity is 41psu in the north due to high evaporation. It decreases southward to 36psu in the south due to the exchange with the Arabian Sea water (see Figure 2.4). When considering the Red Sea at all, [Edwards \(1987\)](#) noted that in february the SST reaches to the minimum value the Sea.

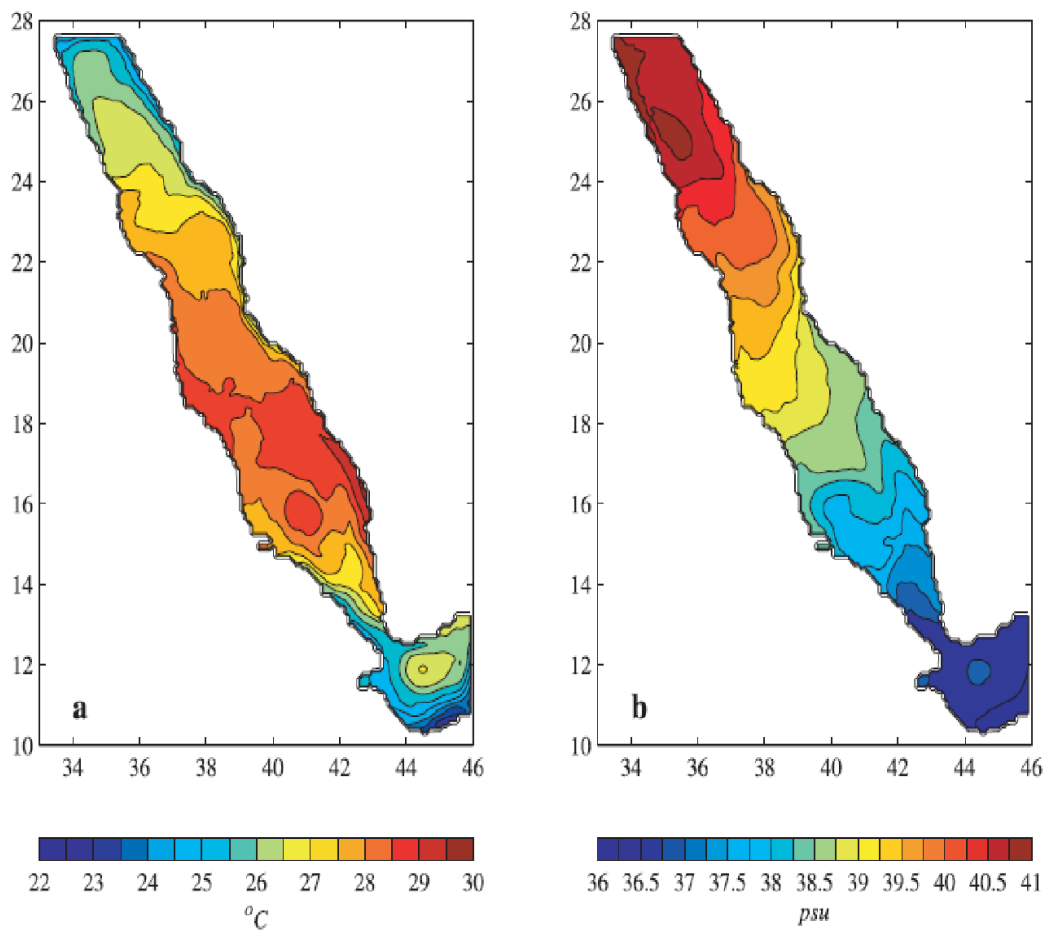


Figure 2.4: Annual mean of sea surface temperature (a), and Annual mean of Salinity (b) to the Red Sea from MICOM simulation (experiment E1, average over the last 9 years of simulation ([Sofianos and Johns, 2003](#))).

2.3.4 The Red Sea nutrients and early studies

The Red Sea appears to be high in nutrients according to [Weikert \(1987\)](#). But the Red Sea water is in general low in the major nutrients such as: Nitrate, phosphate, ammonium and silicates. The north of the Red Sea has low nutrients, while the nutrients in the south of the Red Sea are high as a result of the passing water from the Arabian Sea to the south of the Red Sea. According to the distribution of nutrients, the increase of biological activities goes from north to south ([Mishke et al., 1970](#)). Other investigation by [Fahmy \(2003\)](#) stated that the productivity in the Red Sea is controlled by the concentration of phosphate which is related to the salinity and temperature. All studies of phytoplankton in the Red Sea were qualitative that according to [Halim \(1969\)](#). Such as study stated by [Dowidar \(1974\)](#) recorded 237 species of phytoplankton groups. When considering seasonally, the highest biomass was in winter according to [Levanon-Spanier et al. \(1979\)](#). Some study has been done by [Labiosa et al. \(2003\)](#) in the north part of the Red Sea, especially in the gulf of Al-Agaba, the study shows that there was a strong spring blooms rather than the fall bloom. Both of these blooms had a noticeable change in inter-annual variation.

Chapter 3

Data sources and Data processing

3.1 Data sources

We use the data from both satellites and models. The satellites data are Chlorophyll-a (CHL-a), sea surface temperature (SST), photosynthetic available radiation (PAR) and wind. The data of mixed layer depth is from HYCOM models. Table 3.1 shows in details sources of the data and their information. The Data of chlorophyll-a are downloaded from ESA through the website: <http://www.globcolour.info/>, to access full dataset, go to http://www.globcolour.info/data_access_full_prod_set.html. The data of 8-days global are chosen and downloaded from the link: <ftp://ftp.acri.fr/FPS/CHL1/MERGED/GSM/2005/8DAYS/>. The data of sea surface temperature (SST) are downloaded from the NOAA through the website: <http://www.nodc.noaa.gov>.

Photosynthetic available radiation data are downloaded from NASA through the website: <http://oceancolor.gsfc.nasa.gov/>, to access the data, we used the link <http://oceancolor.gsfc.nasa.gov/cgi/l3>. Wind data were downloaded from NOAA, the website: <http://www.esrl.noaa.gov/psd/data/> is used to download the data in association with (Abdirahman Omer, Bjerknes, 2011). While mixed layer depth data were downloaded from a model through the website: <http://hycom.org/> in association with (Anton Korosov, NERSC. 2011).

3.1.1 Download of data with WGET

3.1.1.1 Chlorophyll-a and sea surface temperature

We started to download the chlorophyll-a data through the following steps:

Section 3.1. Data sources

Table 3.1: Satellites and model data with their units, sources, covering areas, frequency. CHL-a is chlorophyll-a, SST is sea surface temperature, PAR is photosynthetic available radiation and MLD is mixed layer depth. While S.R and T.R are spatial resolution and temporal resolution, respectively.

Variable	unit	sources	S.R	T.R
CHL-a	mg/m ³	ESA	4 km global	8 days 1998-2009
SST	°C	NOAA	8 km global	8days 1998-2009
PAR	Einstein/m ² /day	NASA	9 km global	8days 1998-2009
Wind	m/s	NOAA	2.5 degree	daily 1998-2009
MLD	m	HYCOM.org	1/12 degree	daily 2003-2007

- Open the website which at <http://www.globcolour.info/>.
- Access the full product dataset by using the user name and the password which were written in the bottom of the page: http://www.globcolour.info/data_access_full_prod_set.html.
- To access the 8 days data, we use the following link: <ftp://ftp.acri.fr/FPS/CHL1/MERGED/GSM/2005/8DAYS/>.
- In the command mode and with Wget software using the link above, the data was downloaded for the years from 1998 to 2010.
- To download the SST data, the same commands are used, the only difference is the website used to download the data, which is from ftp://podaac.jpl.nasa.gov/sea_surface_temperature/avhrr/pathfinder/data_v5.

3.1.1.2 Photosynthetic available radiation(PAR)

They data of PAR are downloaded through some step:

- For manual download, we used Mozilla Firefox with the link: (<http://oceancolor.gsfc.nasa.gov/cgi/13>).
- In the browser and by using the key combination "CTRL +U", a window will appear which contains the data source.

- We copy all inside the new window and paste it to Excel file. Then, we sort the data from $(A) \rightarrow (Z)$.
- We copy the lines that start with "http :/" and end with "bz2><img" and paste them in a notepad file. We delete the phrases "href=" and "><img" from the all lines.
- The notepad file is then saved in the folder containing Wget.exe program.
- In the command mode, run the following: (`Wget.exe -i sample.txt`).

3.2 Data processing

3.2.1 Operations in BEAM/VISAT

3.2.1.1 Beam /Visat software

Beam is a professional software to analyse raster data. It has many tools to visualise and even process the remote sensing data. It was originally developed to facilitate the utilization of image data from Envisats optical instrument.

Now Beam deals with other raster data such as GeoTIFF and NetCDF in addition to other format sensors like MODIS, AVHRR, AVNIR, PRISM and CHRIS/Proba. For more information see (<http://www.brockmann-consult.de/cms/web/beam/>).

BEAM/VISAT software has many tools to analyse figures and even extract the data from them (see Figure 3.1). For instance, we choose six buttons to describe some tools available in this software. These buttons are:

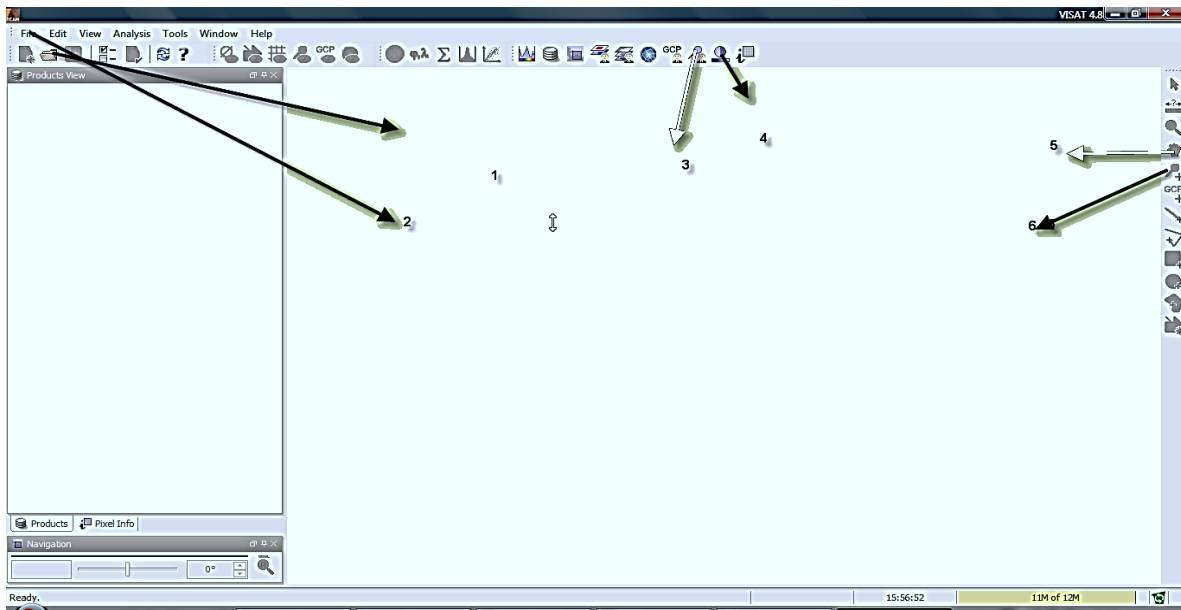


Figure 3.1: Beam/ ViSAT software, the program which is used to analyse the satellite data.

- Button no (1) is used to choose and open pictures into the BEAM.
- Button no (2) produces many operations such as saving pictures and exiting the program.
- Button no (3) manages the pins.
- Button no (4) adjusts colours to the picture.
- Button no (5) controls manipulating the picture.
- Button no (6) adds the pins.

3.2.1.2 Showing the map in the Beam

We started the work in the VISAT/BEAM by opening the pictures from the year 1998, in the imported data, the CHL-mean was chosen. The opened pictures were zoomed in to the area of the Red Sea (see Figure 3.2).

For each year, 46 pictures of CHL-a were opened (which are the picture of all the weeks during the whole year) and same work was done to the SST and PAR data.

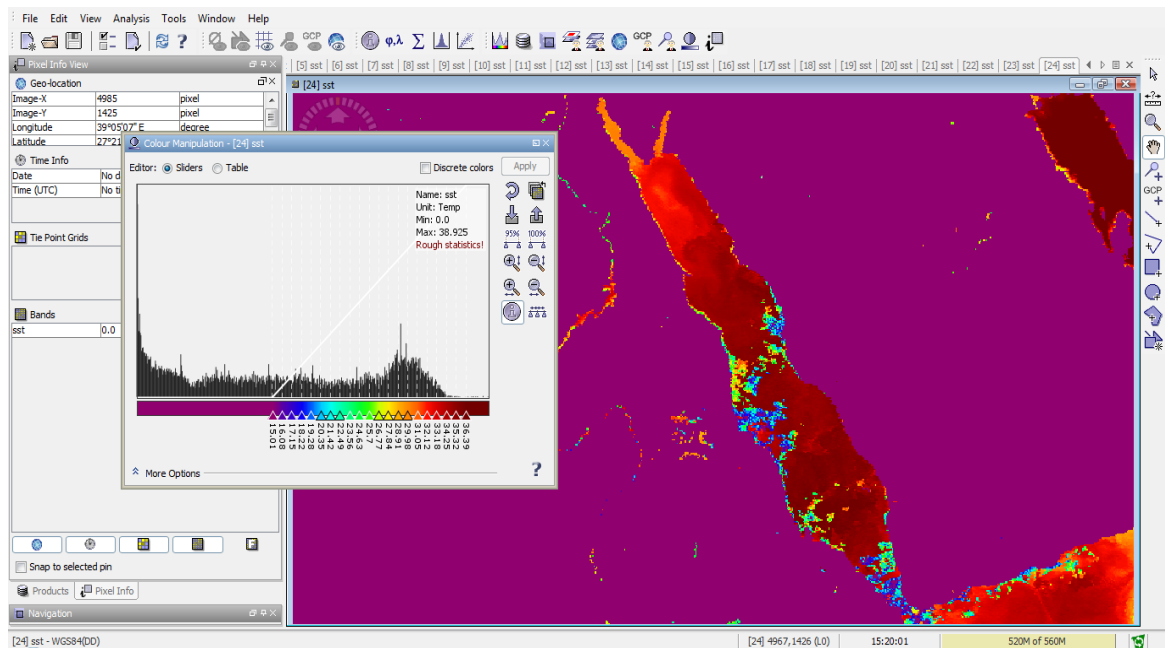


Figure 3.2: the zoomed map of the Red Sea. The SST picture shows the map of the Red Sea on BEAM/VISAT.

3.2.1.3 Distribution of pins in the three zones

To cover all the zone we had to distribute pins which are the tools for extracting pixel values from raster data. for each 50 pins were distributed carefully in each zone to cover the whole area (see Figure 3.3). pins from 1 to 50 covered the north zone, from 51 to 100 covered the middle zone and the pins from 101 to 150 covered the south zone of the Red Sea.

each pin is 1 km². The file of each pins through the three zones was saved carefully with a wise name to use it later.

The PAR file with the pins was created and saved in using different way. As the data of CHL-a and SST are from one satellite, the pins for each zone are in similar places on the map. In PAR, we needed a converter to put these pins in the same place where CHL-a and SST were, and by using Excel file to convert these pins, this file was managed in collaboration with (*AntonKorosov*, NERSC, 2011).

3.2.1.4 Extract the pin values

The CHL values were extracted from the pins through the following steps:

- The picture of specific week was opened.

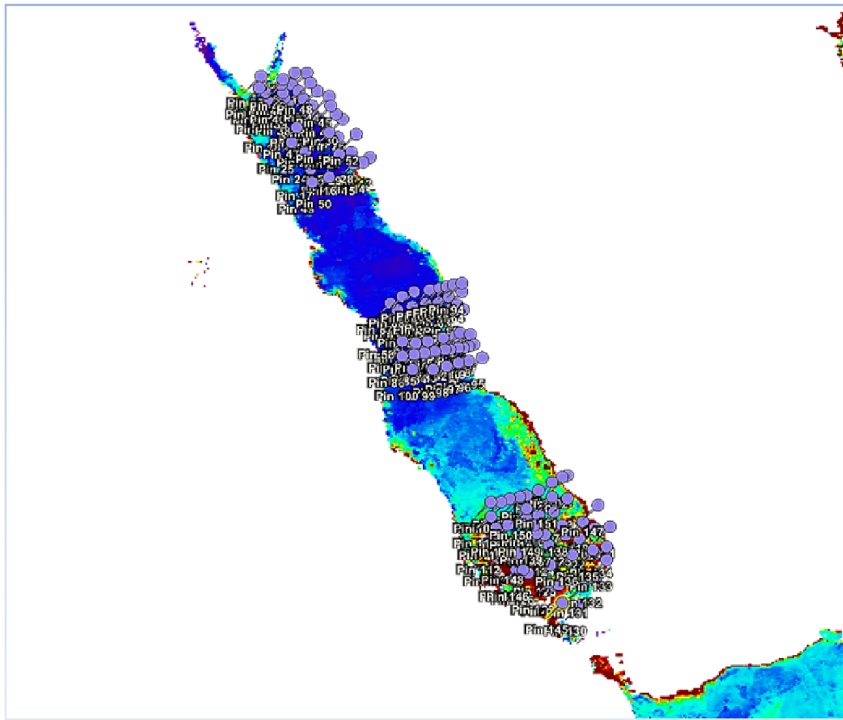


Figure 3.3: Map shows the distributions of the pins in the three zones of the Red Sea, for each zone, 50 pins were distributed carefully to cover the whole zone.

- the files which contains pins for the three zones were imported.
- From the buttons which were in the pins window, the button of filter was pressed and the CHL-mean was chosen.

3.2.2 Operations on Excel

When the data imported to the Excel sheet, we did many steps to the data to be ready for using later. This step are:

- The file which contains pins value and information for the three zones were imported to an Excel sheet.
- The imported data were contain many information such as the name of the pin, logitute and latitute of each pin in addition to the value of CHL1-mean. All these information were removed and left only the values of CHL1-mean.
- The extracted data in the Excel file were separated into three zones according to the zones (North, Middle and South), then quality control for each pin was

done to the CHL-a data by deleting all suspicious values which had no data (NaN).

- Due to the bad quality of the data in the year 2000 in the north zone, the data had to be removed.
- The SST quality control was done to the data in the Excel sheets for each year and each zone. In the bottom, the mean and standard deviation (STDEV) were calculated, then the mean and STDEV were created, they were some values had to make the value of the STDEV higher than even 3, the quality control was done by deleting these values until STDEV became less than 1 (see Figure 3.4).

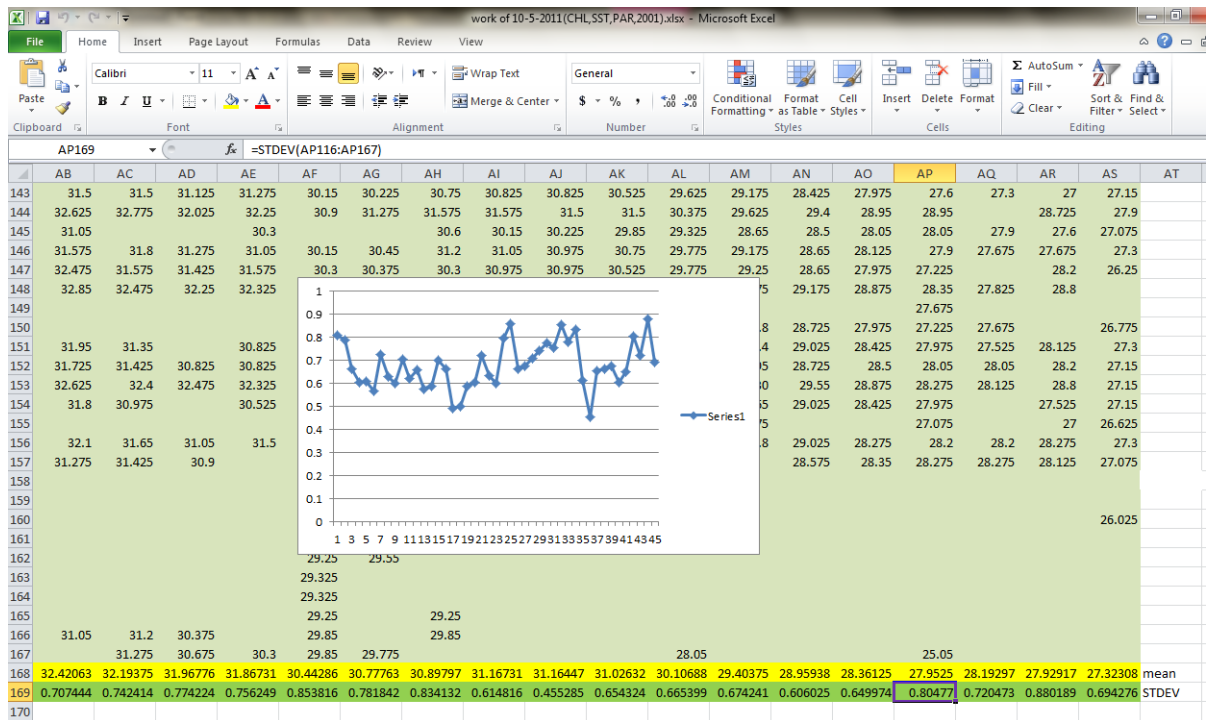


Figure 3.4: Illustrates the SST quality control, the columns are the weekly SST data while the yellow and green rows are the mean and STDEV, respectively.

3.2.2.1 Average Data and Anomalies

For each parameter, after dispersing the data to new excel sheets, statistically operations were done by calculating three mean values and one anomaly:

- (1) Spatial average using (mean of the 50 pins in each zone).

Section 3.2. Data processing

- (2) Smoothing the data by calculating Monthly mean using the weekly averages calculated in step (1) (see figure3.5).
- (3) For **interanuul** variation, monthly climatology (mean of the years from 1998 to 2009) was calculated.
- (4) Each month was subtracted from monthly climatology: for each year (2)-(3).
- (5) For more analysis, the winter months of anomalies were calculated and plotted. Then each correlation was calculated between CHL-a with these physical parameters by using Excel.
- (6) For additional analysis, the correlations between CHL-a of the monthly means and the anomaly means were calculated.

	X	Y	AC	AD	AE	AF
1						
2						
3						
4		date	avg SST	avg PAR	avg MLD	avg WIND
5		01-01-1998	28.16925084	36.6397712		3.820822338
6		02-02-1998	27.73275108	45.0871877		4.231082903
7		06-03-1998	27.72125369	53.04376695		4.744782847
8		07-04-1998	30.46950097	56.00300585		4.288721881
9		01-05-1998	31.26300098	57.49591205		5.209143253
10		02-06-1998	32.27587611	57.26124628		4.809511113
11		04-07-1998	34.16203007	56.6791529		4.970682825
12		05-08-1998	33.72298879	52.86198775		4.063918847
13		06-09-1998	33.59888374	47.77282215		4.708550628
14		08-10-1998	32.990626	41.41591285		4.286335638
15		01-11-1998	32.31262599	36.48198875		3.861751872

Figure 3.5: the smoothed data (monthly mean) for CHL-a and other physical parameters. MLD data started from 2003.

Chapter 4

Results and discussion

4.1 the North zone

The Dynamics of chlorophyll-a in the north zone vary during the year. Figure 4.1 shows the weekly data of chlorophyll-a (CHL-a) concentration. CHL-a is always

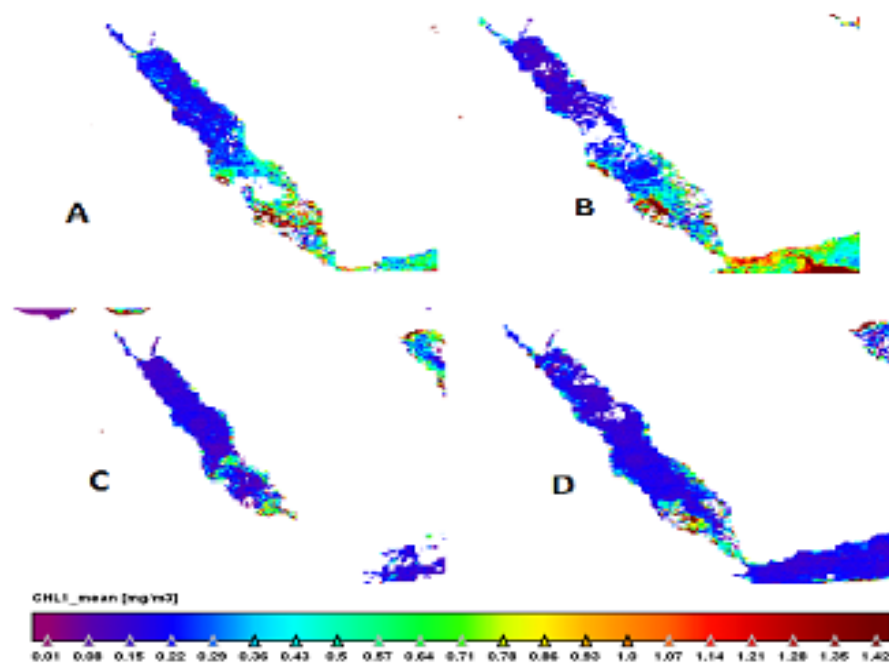


Figure 4.1: Illustrates the CHL-a pictures in different seasons in 2001. A and B pictures during winter. A in January and B picture in December. While the C and D during the summer. C in June and D in April. The pictures show that the blooms were in winter.

Section 4.1. the North zone

high during winter months see Figure 4.2, which is from late November to the end of March in the next year. Maximum value is always in January ($0.3\text{mg}/\text{m}^3$). The weekly plot is not clear enough to see the boundaries between the blooms time.

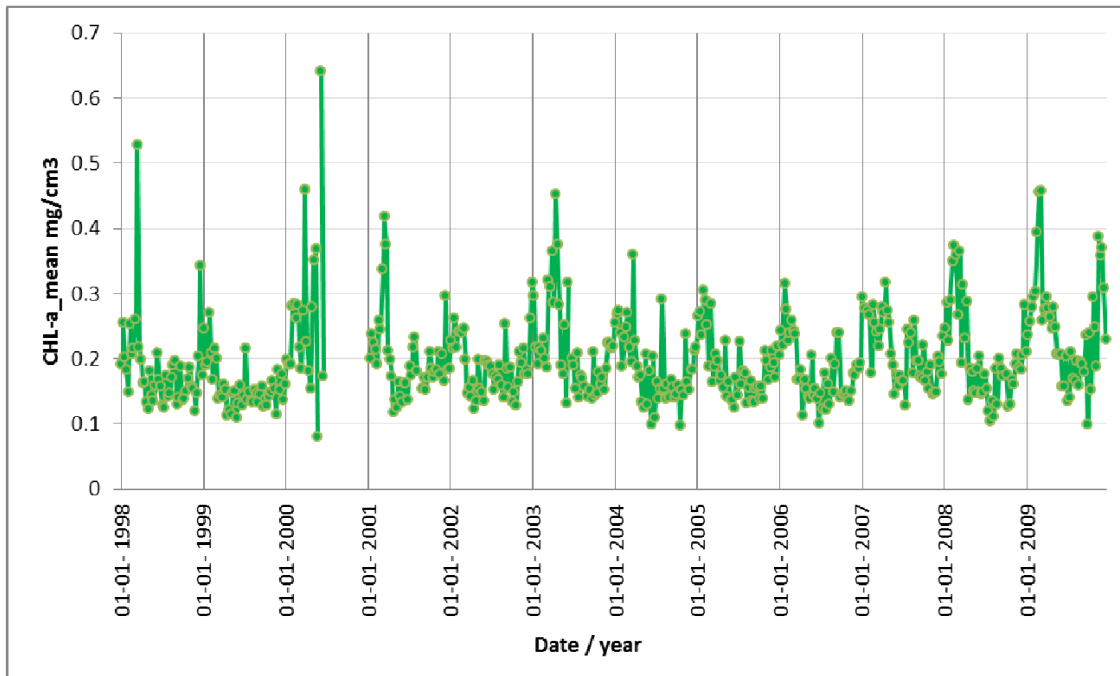


Figure 4.2: weekly concentration of surface Chlorophyll-a (mg/m^3) from the period 1998 until 2009 in the north zone of the

The smoothed plot (monthly concentration of chlorophyll-a) shows clearly Figure 4.3. Seasonally, the chlorophyll concentration is low during summer months (May to October), the lowest value is different from year to year, where is the average low value is ($0.14 \text{mg}/\text{m}^3$). In winter, the concentration reaches to the high values which vary from year to year, the average maximum value is ($0.26 \text{mg}/\text{m}^3$).

some years in monthly plot show different peaks than others and these years are: 2003, 2007, 2008 and 2009. In 2003 the blooms have more than one peak, meaning that it occurs three times during the winter and ends in May, yet the blooms started in November and ended by the end of March for the other years. Also the 2007 shows two peaks which means there is also a double bloom.

In 2008 and 2009 and even in 2003, the maximum value of CHL-a is higher than other years during blooms. 2009 is a high value during blooms which is ($0.4 \text{mg}/\text{m}^3$), while lower value in 1999 is comparable with other years such as 2001, because the

blooms always starts two months before, with unclear data and the end of 2000, still 2001 shows high values when it compares with other years. The trend line shows that the chlorophyll concentration increases during the all years ($R^2=0.0607$). 2009 has a high CHL-a value more than other years, thus the trend line became stable ($R^2=0.0182$) when the 2009 was removed.

4.1.1 Physical parameters and their effects on the CHL-a

The Physical parameters which I have determined to have an effect on CHL-a are: sea surface temperature (SST), photosynthetically available radiation (PAR), mixed layer depth (MLD) and wind. SST as shown in Figure 4.4 always increases during summer from April to October where the high value is always about (32°C) in July, then it goes down during winter until (25°C) in January which shows a minimum value. Furthermore, it looks different when it is compared with CHL-a, the plot shows that the higher values are in 2001 and 2009 where the value of R^2 in trend line changes from ($R^2=0.038$) to ($R^2=0.0005$) by removing these two years.

The plot of PAR shows that the PAR always increases from January until max values which are about ($62 \text{ Einstein}/\text{m}^2/\text{day}$) always in July, then the plot goes down to the minimum value in December ($29 \text{ Einstein}/\text{m}^2/\text{day}$) (see Figure 4.5). For the last years 2008 and 2009, the high values of PAR in winter in April and February, respectively.

For the years which have different CHL-a values other than as shown in 1999, 2003, 2007, 2008 and 2009, the plot of SST and PAR does not show special variation during these years. These years vary whereas, in other years, the chlorophyll-a increases during summer and decreases in winter.

Mixed layer plot in north does not produce useful information. With bad data the plot miss leading to anything, we cannot say anything when we want to know the effect of MLD into CHL-a (see Figure 4.6).

The dynamics of wind speed is the same as the dynamics of SST and PAR, it increases from mid of March until May and June which is max value (4.4 m/s) then it decreases until the end of November where it has a minimum value (3.0 m/s) see Figure 4.7.

SST and PAR have same variation. Both of them increased until the middle of a year (July) always, then they decrease by the end of the year meaning that the SST, PAR

Section 4.1. the North zone

and wind have negative correlation with CHL-a.

The trend line shows the wind is stable whole years and that is shown from the value of $R^2=0.0004$.

The last three years 2007, 2008 and 2009 have low values of wind speed, the wind speed if they compare with the speed during all years.

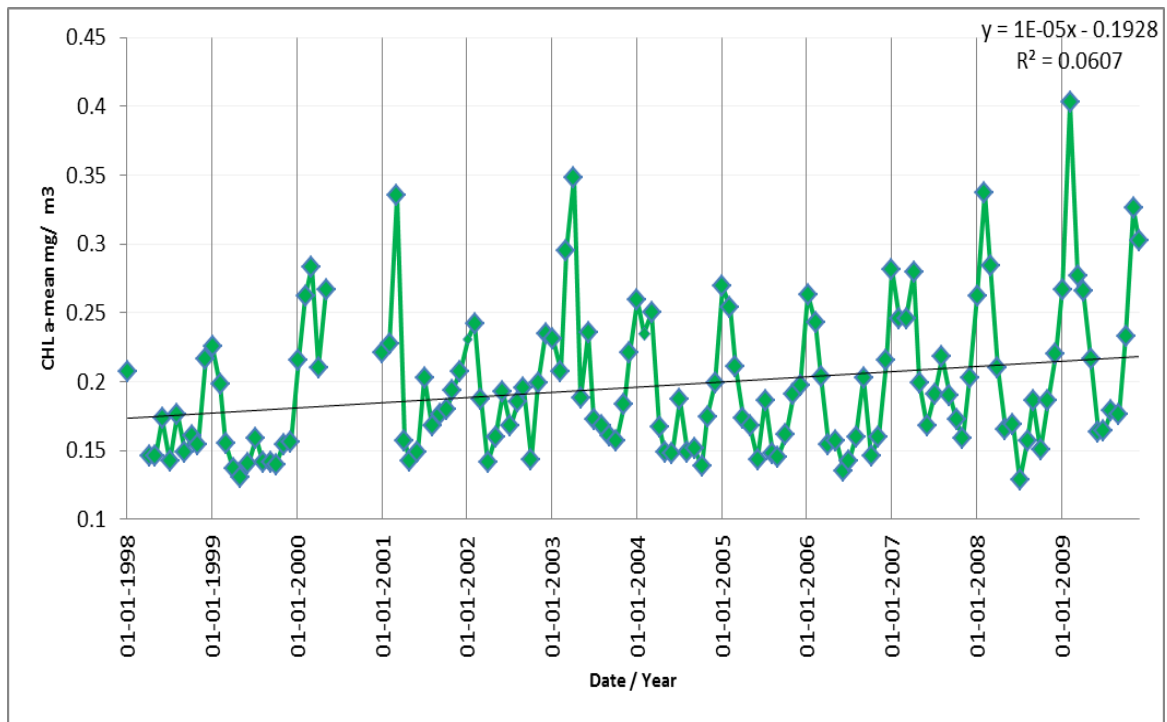


Figure 4.3: Monthly mean concentration of CHL-a mg/m^3 to the all years from year 1998 until 2009 in the north zone of the Red Sea.

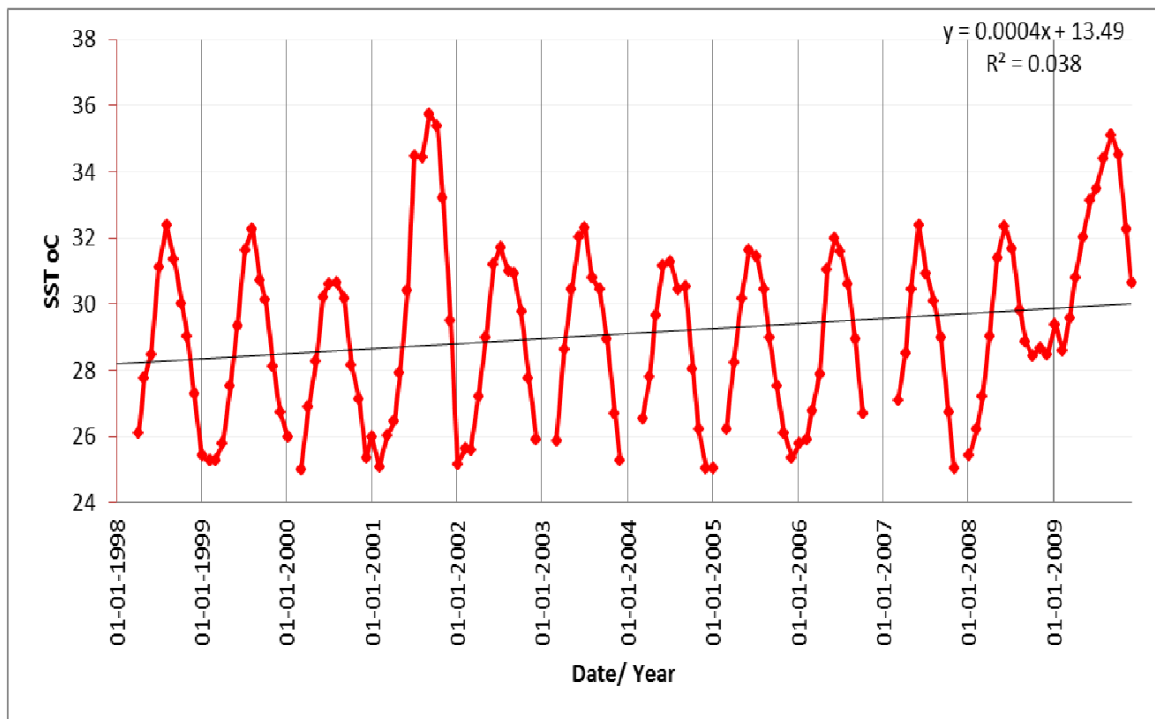


Figure 4.4: Monthly mean of the Sea Surface temperature for the year from 1998 until 2009 in the north zone of the Red Sea.

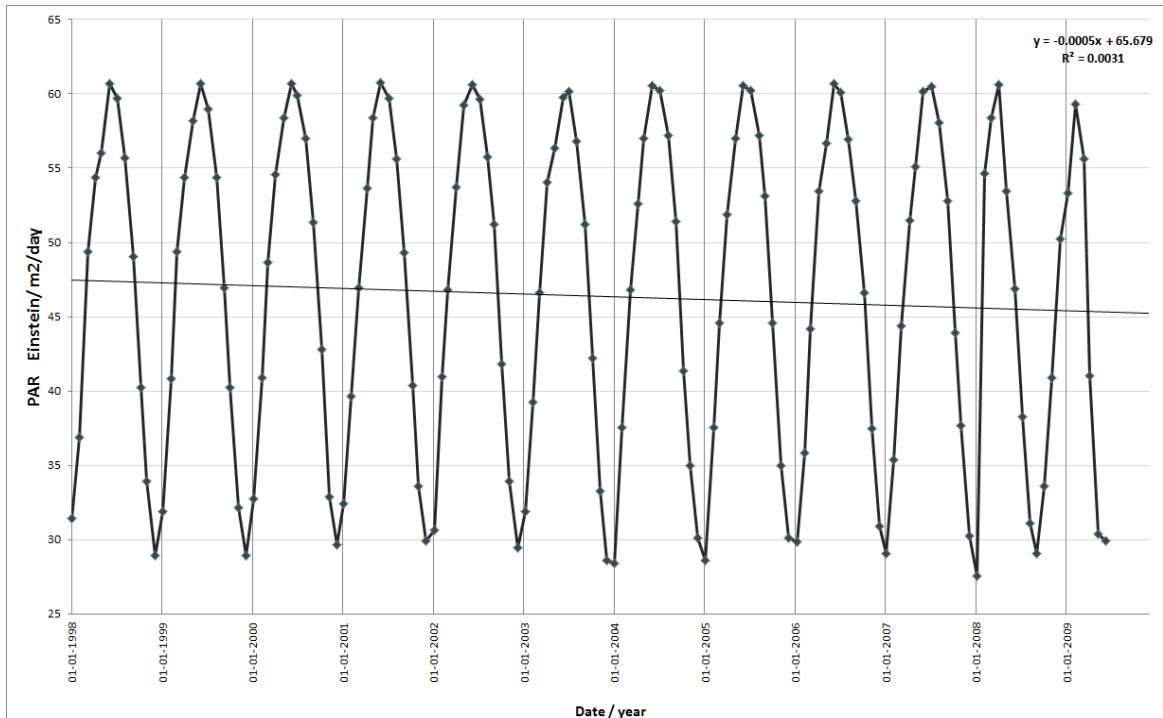


Figure 4.5: Monthly mean of Photosynthetically available radiation, from the period 1998 until 2008 to the north zone of the Red Sea.

Section 4.1. the North zone

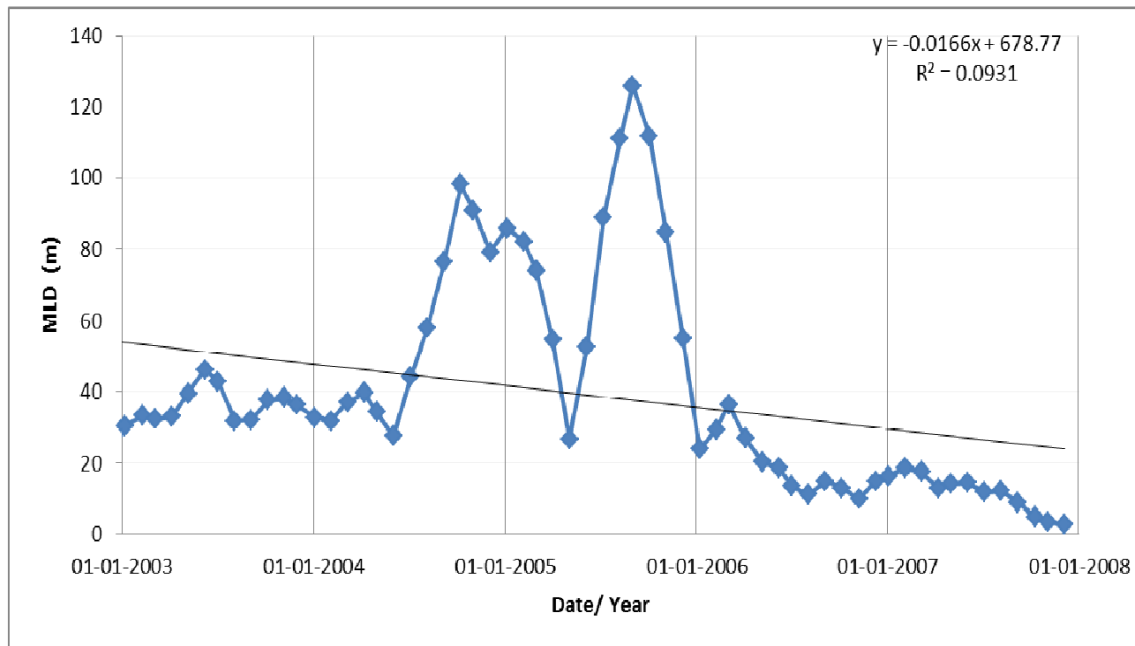


Figure 4.6: Monthly mean of mixed layer (m)depth from the period 2003 until 2007, north zone of the Red Sea. The figure shows unclear date specially 2005 and 2006.

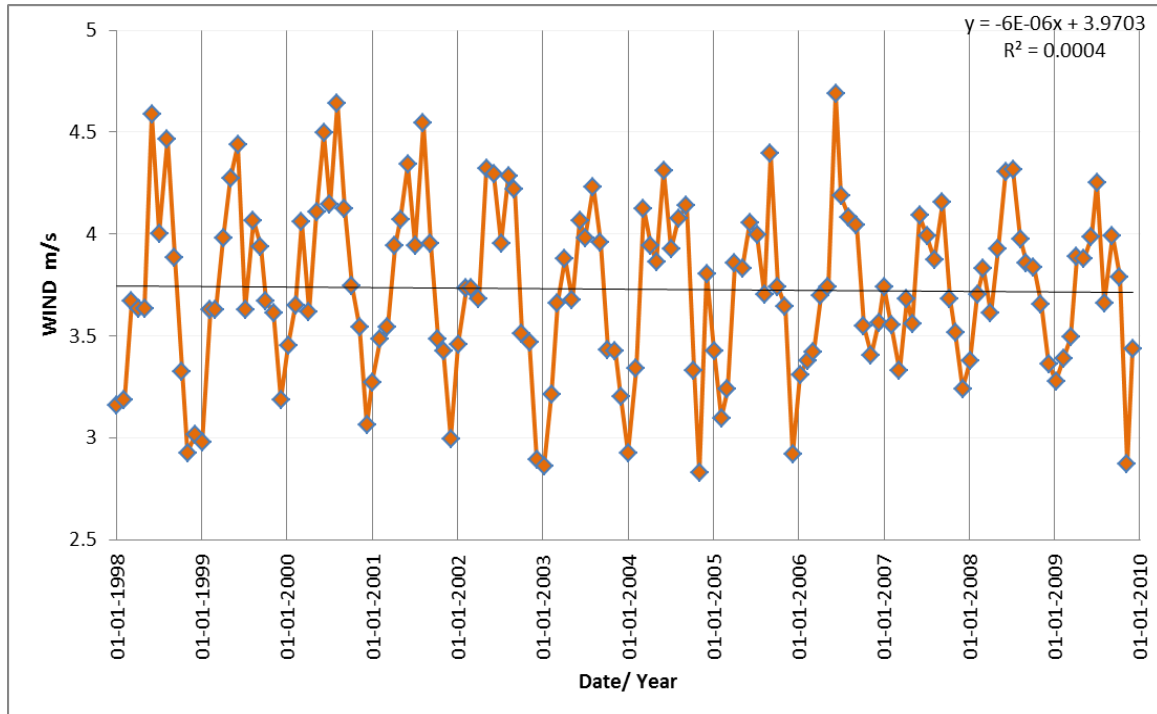


Figure 4.7: Monthly data of wind (m/s) for the period from the period 1998 to 2009. North zone of the Red Sea.

Table 4.1: Monthly Correlation of CHL-a with other physical parameters (SST, PAR, wind and MLD) north zone of the Red Sea.

correlation	SST	PAR	MLD	Wind
CHL-a	-0.429	-0.200	-0.159	-0.356

Interannually, the plot of anomaly show the variation of CHL-a in winter months is from (-0.035) to (0.028). The plot of CHL-a and other physical parameters show difference variation and correlation values between months and anomalies data. SST and PAR totally changed from no correlations to positive correlation between them and the CHL-a 0.722 and 0.936 for SST and PAR respectively. That appears from the plot and correlation. While MLD, the correlation negatively weak (-0.159). It becomes more negative (-0.567). In wind there still no correlation even the value goes from negative in monthly data (-0.356) to positive in anomalies (0.157) see Figure 4.8) and Table 4.2.

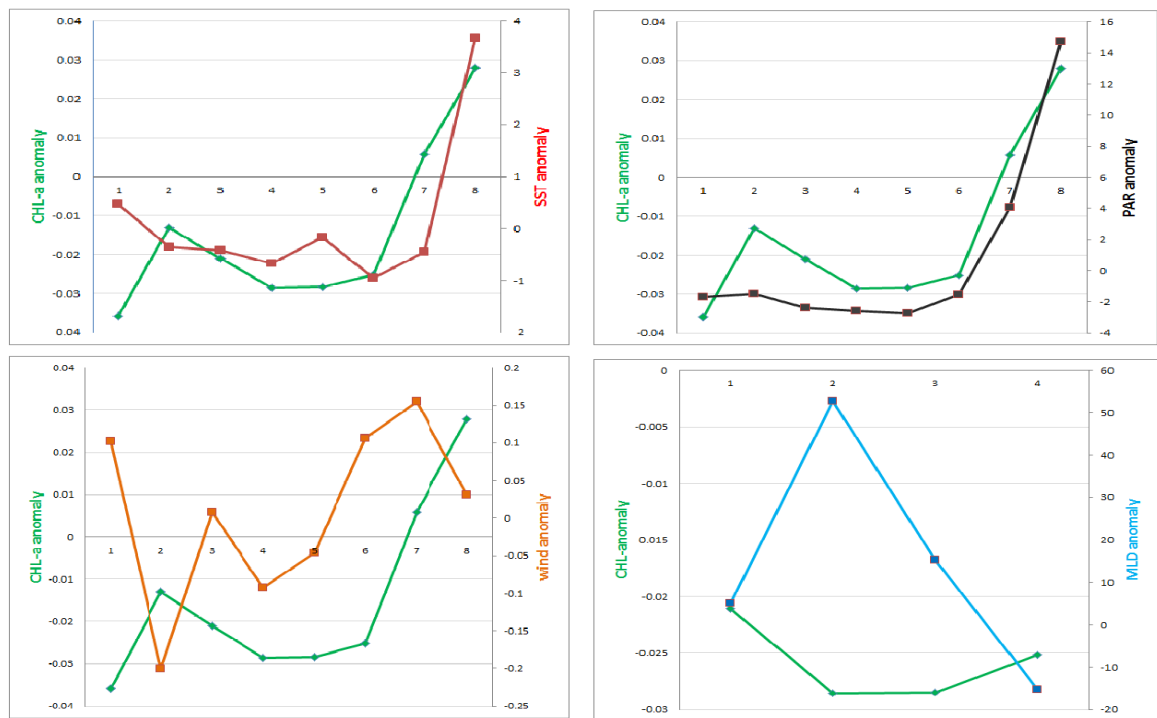


Figure 4.8: Monthly anomalies plot of CHL-a with the physical parameters in the north zone of the Red Sea, the different between each month and the month climatology

Generally, The chlorophyll concentration is low in the north zone of the Red Sea, according to [Acker et al. \(2008\)](#) who studied in the northern zone of the Red Sea from

Section 4.2. the North zone

Table 4.2: The anomalies correlations of CHL-a with other parameters in north zone of the Red Sea. The table contains values PAR and SST shows high values of correlation.

corrlation	SST	PAR	MLD	Wind
CHL-a	0.722	0.936	-0.567	0.157

the period of 1998 to 2004. Where the concentration of CHL-a was stated as lower than (0.2 mg/m^3) far from the coast and can be compared to what my results show. [Kotb et al. \(2004\)](#) stated that the sea surface temperature and nutrients decrease northward in the Rea Sea and that what is monthly data of chlorophyll-a data show in the north of the Red Sea.

the Red Sea lies in the tropical region and light is always there throughout the year. The chlorophyll blooms should therefore be controlled by nutrients. The source of nutrients in the north of the Red Sea should either MLD or wind. MLD plays an important factor in providing the nutrients which phytoplankton need for the photosynthesis process as it brings nutrients from deep water to the euphotic zone where phytoplankton lives. Moreover, with little good data shown by the mixed layer, it is difficult to say whether or not the mixed layer was effected in the blooms in the north of the Red Sea.

During the winter the south zone of the Red Sea receives the Arabian Sea water which is pushed by the south-west monsoon. The high nutrients pass through the Red Sea until they reach to the north, by crossing all this area the nutrients are consumed by phytoplankton and a little amount of nutrients arrive to the north of the Red Sea and therefore why chlorophyll concentration in the north zone of the Red Sea was low.

For the years which had high values of CHL-a, 2003, 2007 2008 and 2009, SST, PAR and wind plots did not show special variation, only in 2009 was the SST high but all of the monthly correlations between CHL-a and SST are shown to be weak see [Table 4.1](#).

Eventhough in the two years of PAR 2008 and 2009 the maximum values of PAR were during winter, but we cannot say that the last two yeas in CHL-a controlled by the PAR because the high values of CHL-a abd PAR were in different month in winter.

Winter months anomalies in the north of the Red Sea came out with different results. the high varaitions in anomalies plot means that the high values during the years 2003, 2007 2008 and 2009 were responsible for this range. The year 2009

controlled the shifting of the trend line through all years and this was seen when 2009 was removed and the value of R^2 became less than it was.

4.2 the Middle Zone

The Same work was done to the middle or (center) zone, by plotting monthly CHL-a and other physical parameters during all years.

When considering the Chlorophyll-a seasonally, dynamics in the middle (center) zone in the Red Sea is the same to the north during blooms time which is in winter

The blooms start earlier on the mid of October and reaches the maximum value in December (0.24 mg/m^3). And then it decreases until the end of March when the blooms end at (0.12 mg/m^3).

During these twelve years, the years of 2006, 2008 and 2009 stand out with higher values than other years. 1998 and 2005 are different, the blooms occurred in summer which was unexpected.

2009 has a double blooms as both of the blooms start and end in winter. One of them started and ended earlier than the other one. The other two years 2006 and 2008 and 2009 have high values of chlorophyll-a during the blooms 0.34 mg/m^3 , 0.28 mg/m^3 and 0.27 mg/m^3 , respectively (see figure 4.9).

The trend line shows that the chlorophyll in the middle zone of the Red Sea increases normally during these twelve years ($R^2=0.0157$) Figure 4.9, when 2008 and 2009 have been removed, the trend line became stable through out all years with ($R^2=0.0009$).

The variation of SST in the middle zone is the same as in the north. SST always increases during summer until July which is the max value (34.2°C), while the minimum value approximately (28°C) in December (see Figure 4.10), which always, observes in December. The SST in the middle is higher than the north, that appears from the average maximum values for each to them, it is (31°C) in the north zone and (34°C) in the middle zone of the Red Sea.

The dynamics of photosynthetic available radiation same as SST, it increases in the same months where SST increases and it reaches the high values almost in June approximately ($57 \text{ Einstein/m}^2/\text{day}$). And by the same way it decreases until December with the minimum value of PAR ($33 \text{ Einstein/m}^2/\text{day}$).

Section 4.2. the Middle Zone

The trend line shows the decreasing of PAR during the years with $R^2=0.0059$ (see Figure 4.11). But at this time it is bigger than that of SST had $R^2=0.0025$ (see Figure 4.10).

MLD looks better than it is on the north zone as we can see the variation between each year and other years even with a limited data (only 4 years) Figure 4.12. It increases in the same way as CHL-a and opposite with SST and PAR. The positive correlation appears between CHL-a and MLD (0.544) see Table 4.3.

The dynamics of wind speed is same as the dynamics of SST. The summer months have high values of wind, while the winter months when the blooms occurring have low values.

Wind speed in the middle shows minimum values for the years 2001, 2002 and 2003 the high value during these years was (4.3m/s). Other years have variation with maximum values (5.4 m/s) in 2005. Even though the last years in CHL-a plot have high values, in the wind for example, and yet there is no correlation between them (-0.005). Some years such as 2005, and 2007 where wind speed reaches to the high values in January, and that occurs during the blooms (see Figure 4.13).

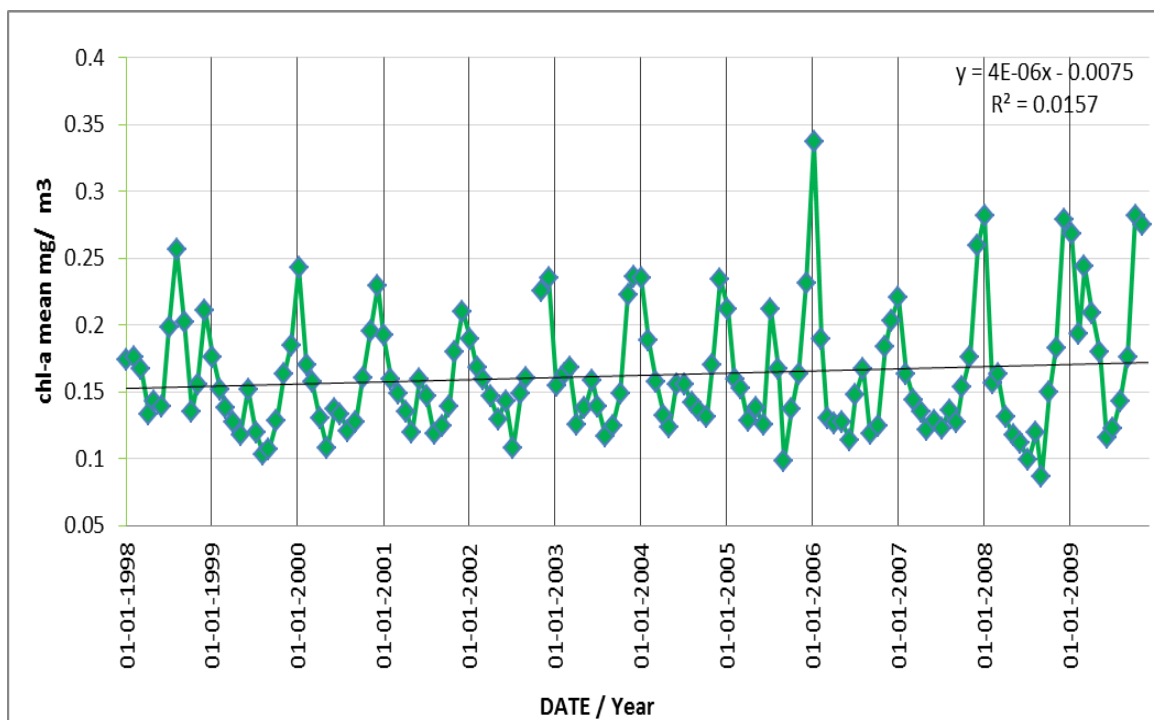


Figure 4.9: Monthly concentration of chlorophyll-a from the period 1998 to 2009 in the Middle zone of the Red Sea.

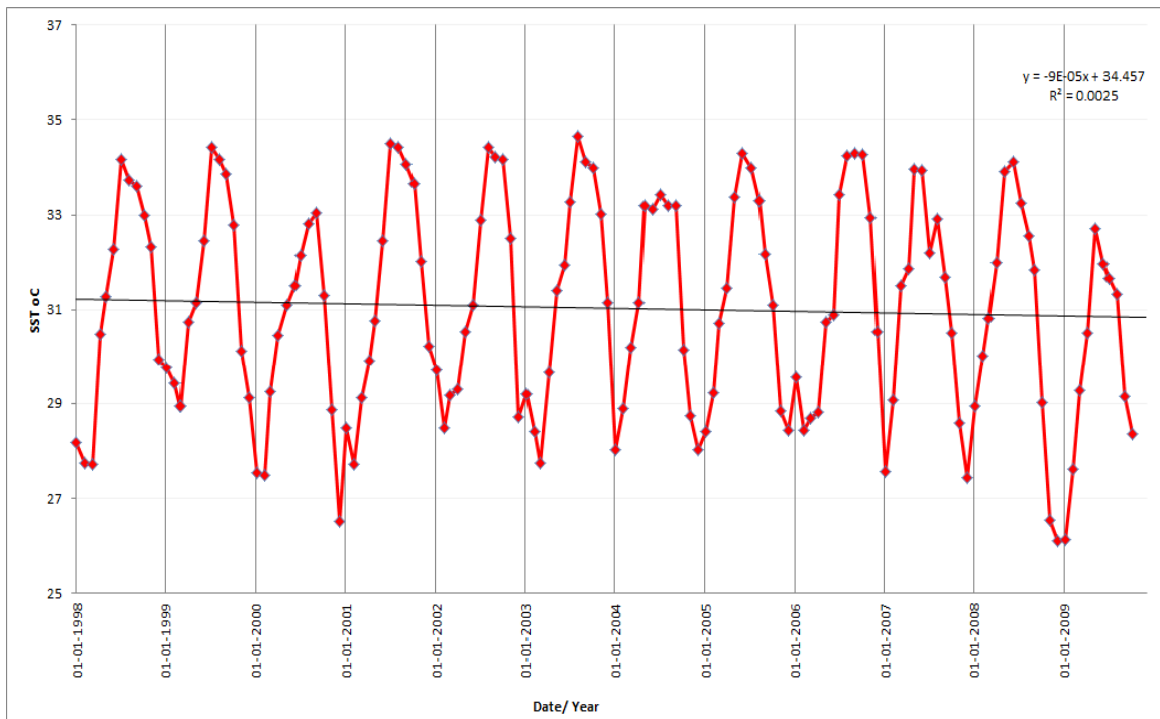


Figure 4.10: Monthly mean of Sea Surface temperature (SST) for the period from 1998 to 2009 in the Middle zone of the Red Sea.

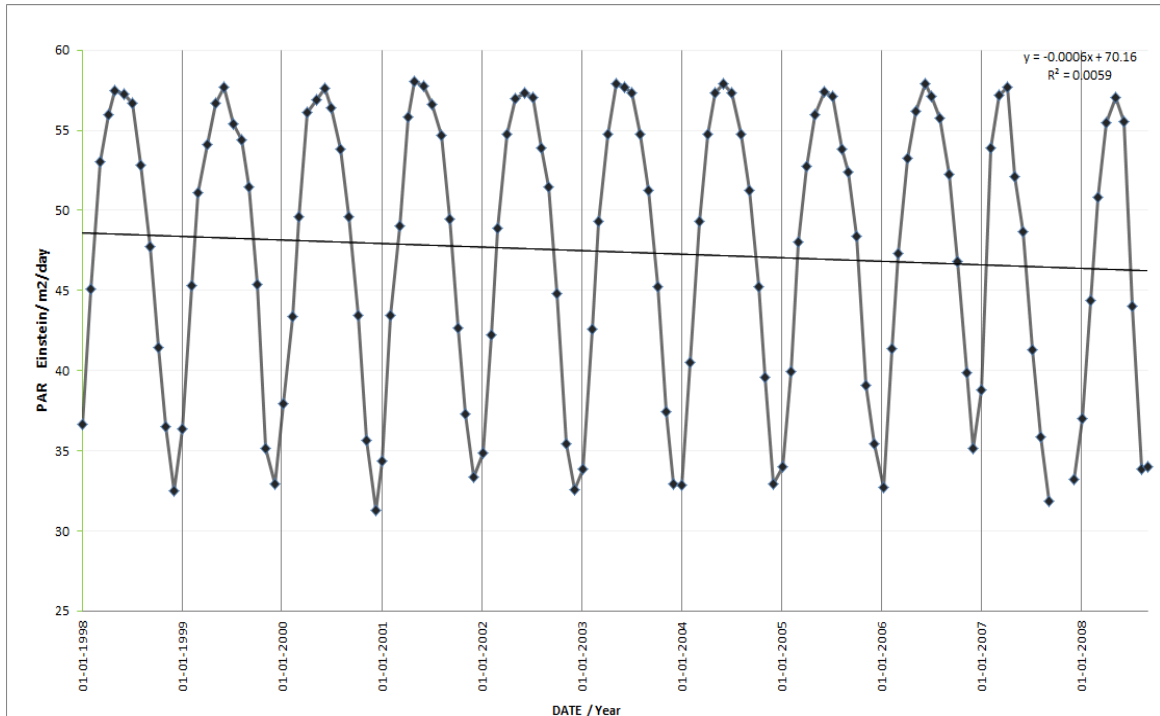


Figure 4.11: Monthly data of Photo synthetically available radiation (PAR) for the period from 1998 until 2009 in the Middle zone of the Red.

Section 4.2. the Middle Zone

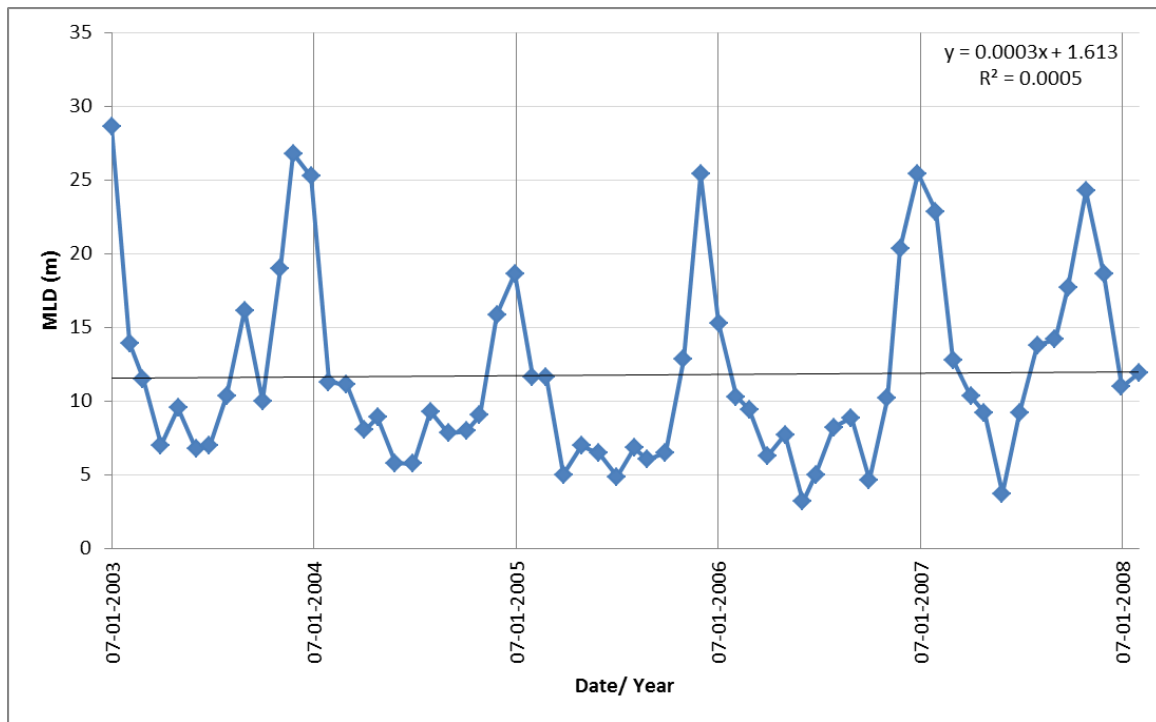


Figure 4.12: Monthly data of mixed layer depth (MLD) for the Period from 1998 until 2009 in the Middle zone of the Rea.

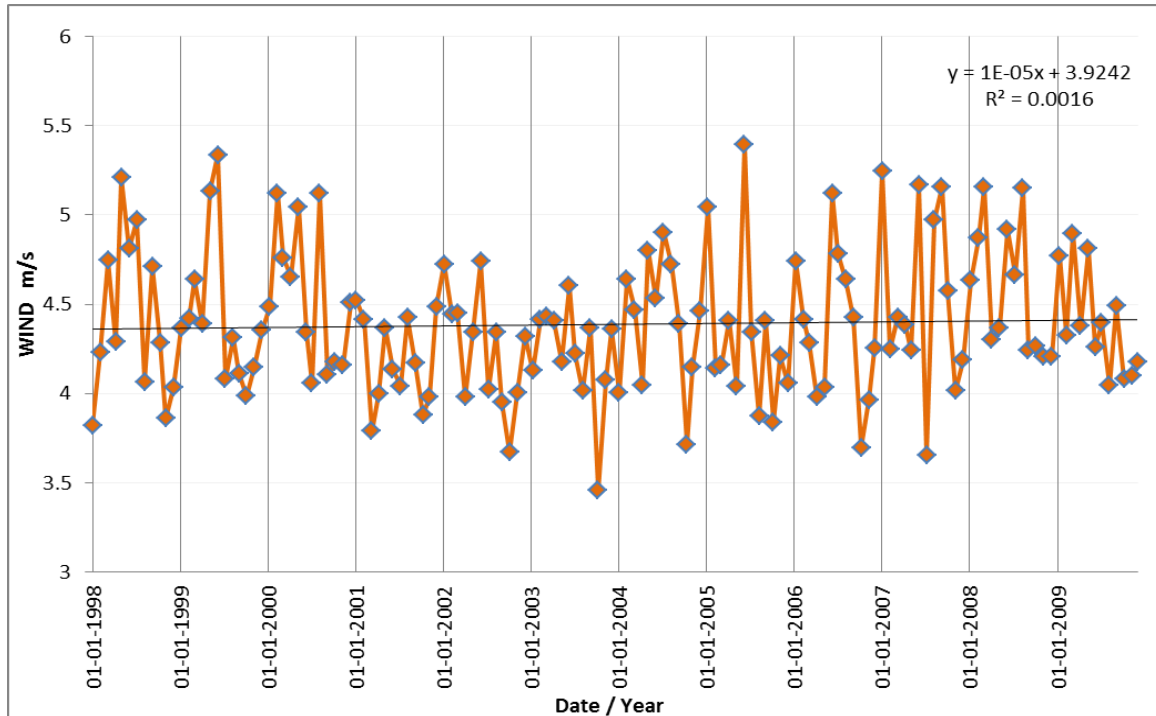


Figure 4.13: Monthly data of wind speed from the period 1998 until 2009 in the middle zone of the Red Sea.

Table 4.3: Monthly correlation of CHL-a with the physical parameters in Middle Zone of the Red Sea. SST is sea surface temperature, PAR is photosynthetic available radiation and MLD is mixed layer depth.

correlation	SST	PAR	MLD	Wind
CHL-a	-0.512	-0.587	0.544	-0.005

Inteannually, in this zone, the variations of CHL-a during whole years was from -0.015 to 0.035. The correlations in the winter Anomalies and monthly have different values of SST and PAR, but they their values still stand out the negative correlation between CHL-a and SST. In the PAR, the value of correlation becomes weak (-0.253) but still shows negative values in both monthly and anomaly see Figure 4.14 and Table 4.4.

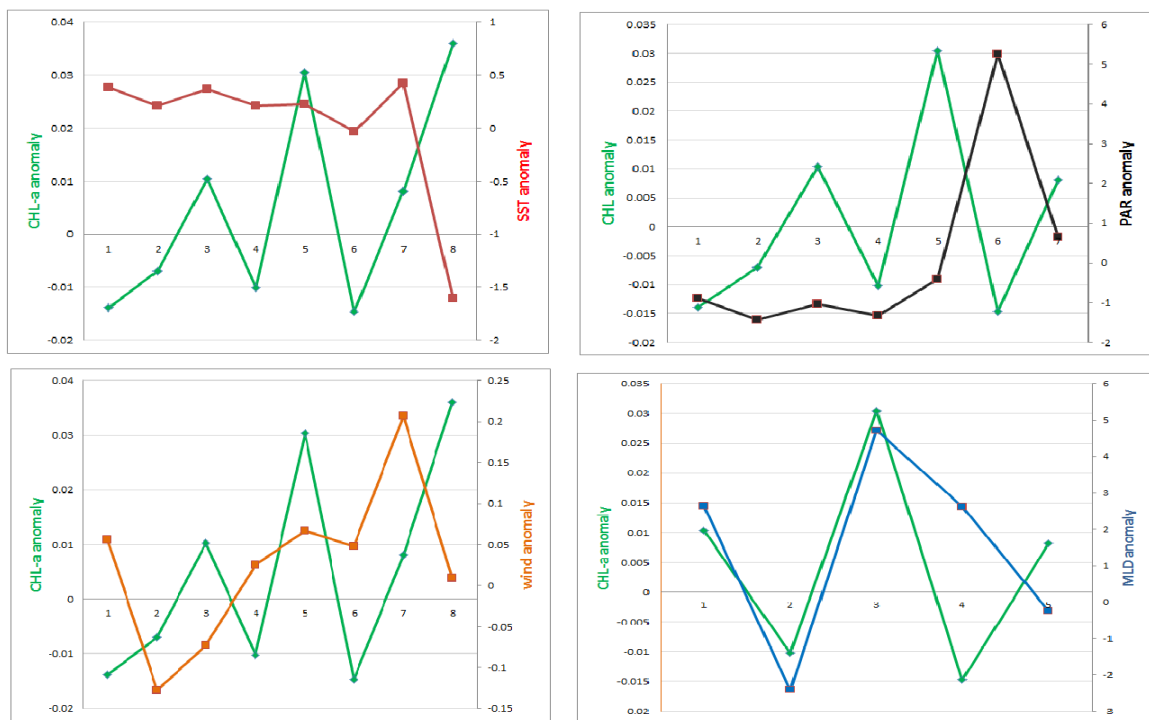


Figure 4.14: Monthly anomalies of chlorophyll-a with other physical parameters during winter months, the plot for the middle zone of the Red Sea.

Table 4.4: Anomalies correlation of CHL with other physical parameters in Middle Zone of the Red Sea

corrlation	SST	PAR	MLD	Wind
CHL-a	-0.566	-0.253	0.591	0.100

The middle zone of the Red Sea shows different plots, for example, the maximum values of CHL-a during the blooms are higher than in the north. The blooms always starts and ends before the end of the year.

The trend line becomes stabilised when the data of 2008 and 2009 are removed, which means these two years shifted the trend line toward these years. SST values in the middle are higher than in the north (Sofianos and Johns, 2002). And that proves the higher value in the middle zone more than the north zone. The result in Table 4.3 indicates that there is a negative correlation between SST and CHL-a variations. Meaning that the CHL-a decreases when SST increases, and the same has been observed between the CHL-a and the PAR.

The weak correlation between the wind and the CHL-a indicates that the wind does not control the CHL-a bloom. The CHL-a blooms during 2005 and 2007 perhaps due to the increase of the wind speed in these years.

The blooms in the middle zone from 2003 to 2007 are controlled by the MLD, which are shown from the plot of CHL-a and MLD. The CHL-a is always high when the MLD is high, the value of correlation between CHL-a and MLD supported that. For the years which have higher blooms values than other years or even have double blooms, the mixed layer is high only in 2006.

The control of CHL-a by MLD is what we expected because the nutrients in the middle zone have to come either from the south or from the bottom of the Red Sea. Since the wind has a weak correlation, the nutrient should only come from the bottom and that is what the MLD shows to be true.

4.3 the South zone

The thing that makes Southern zone different from other zones is: the direct connection between this zone and Arabian Sea. It has high value in chlorophyll than the two zones (see Figure 4.15). The amount of chlorophyll decreases northward. The figure was during the bloom, it shows that the south of the Red Sea is has higher blooms than other zones.

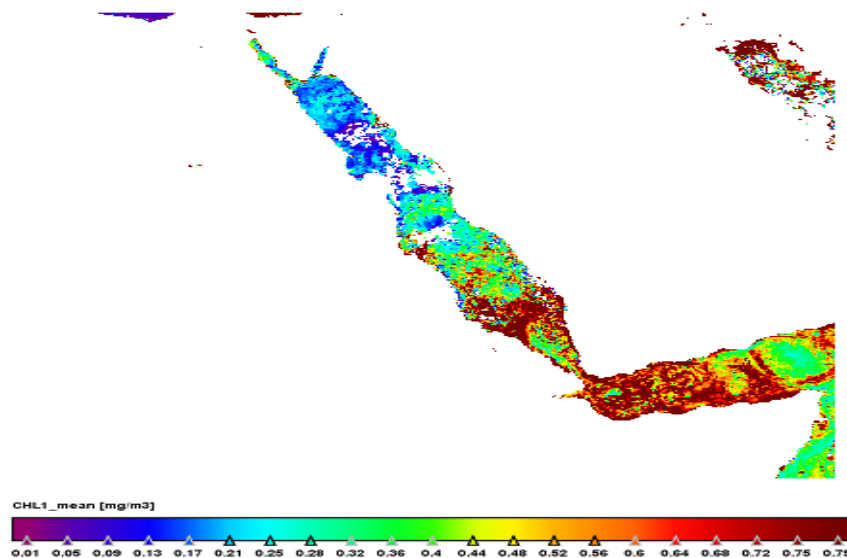


Figure 4.15: picture of january-8 during blooms for the Red Sea and North zone of the Arabian Sea. Showing the high blooms in north of Arabian Sea and south of the Red Sea

Seasonally, The chlorophyll dynamics always starts with the beginning of winter, but in this zone the blooms start in September and end February. The maximum values are in December which is higher than what in other zones ($0.7\text{mg}/\text{m}^3$). Then the concentration decreases until the end of blooms, Figure 4.16.

Some years such as: 1998, 2008 and 2009 observe higher values than other years. From 1998 until 2000, there are many blooms even in summer. The trend line shows that the CHL-a in the southern zone decreases through these twelve years from 1998 until 2009 ($R^2=0.042$).

In the south, SST in the south is higher than other two zones. That from the average maximum value which is (35°C) see Figure 4.17.

Section 4.3. the South zone

The dynamics of sea surface temperature (SST) shows increasing of SST summer months which are from may until September. The high value of SST is stable during the summer months. But almost in August. During the blooms time which SST has the lowest values (29°C). The first three years have maximum values if they compare with others and the trend line decreases during the years until 2009.

Photosynthetically available radiation dynamics are the same as SST. Increases during summer months, (March until September). The maximum value is about (56 Einstein/m²/day) is always in May, then it decreases from November to March which is a minimum values always during December (37 Einstein/m²/day) (see Figure 4.18).

MLD is limited for only 5 years. It increases during winter month which the high value in January >10m. The mixed layer reaches to the high value when the blooms have already occurred (see Figure 4.19).

At the all zones in the Red Sea, wind speed is high during summer and low is winter. The maximum value of Wind speed always in the mid of year almost (4.4 m/s), and the low value in November 3.2 m/s. The Trend line does not observe any change during years while it decreases with a small value is ($R^2=0.0011$) (see Figure 4.20).

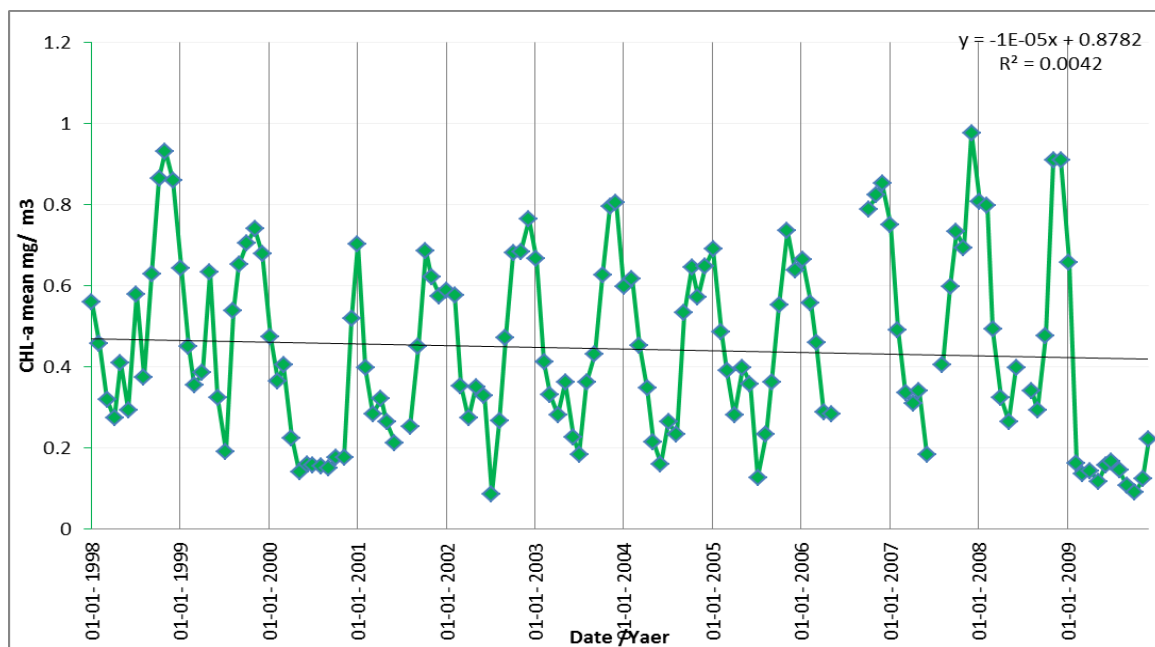


Figure 4.16: Monthly concentration of chlorophyll-a to the period from 1998 until 2009. South of the Red Sea

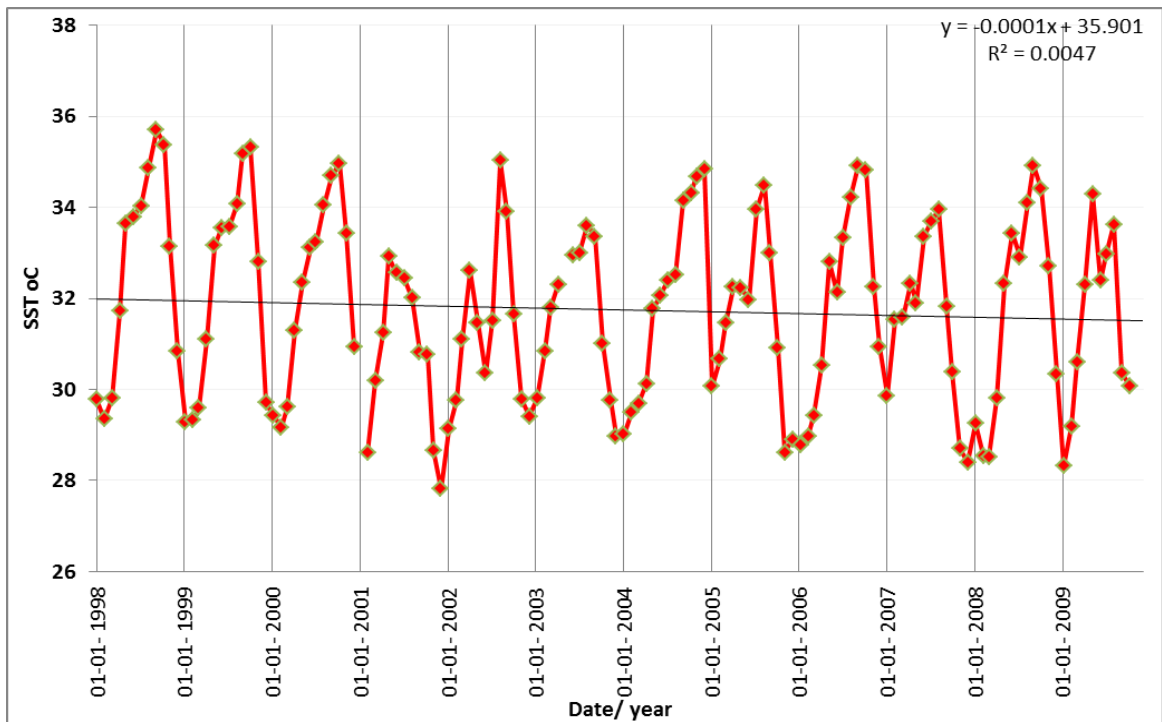


Figure 4.17: Monthly data of sea surface temperature SST, to the south zone of the Red Sea from the period 1998 until 2009.

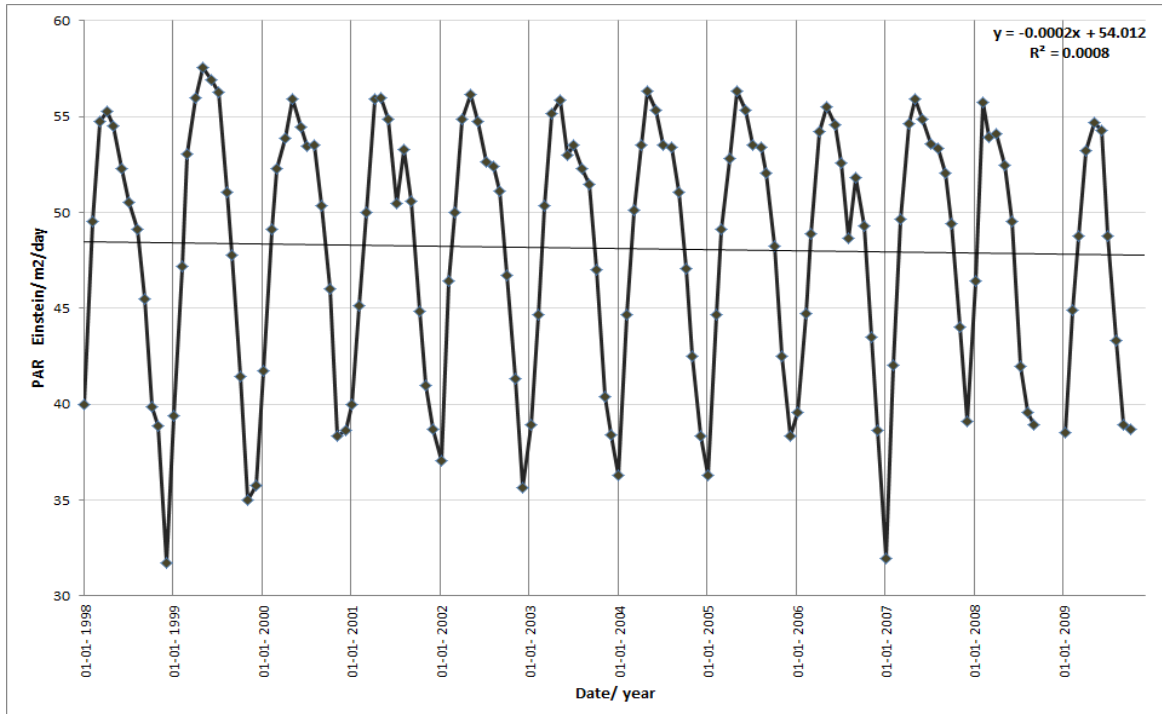


Figure 4.18: Monthly data of photosynthetic available radiation PAR to the south zone of the Red Sea from the period 1998 until 2009.

Section 4.3. the South zone

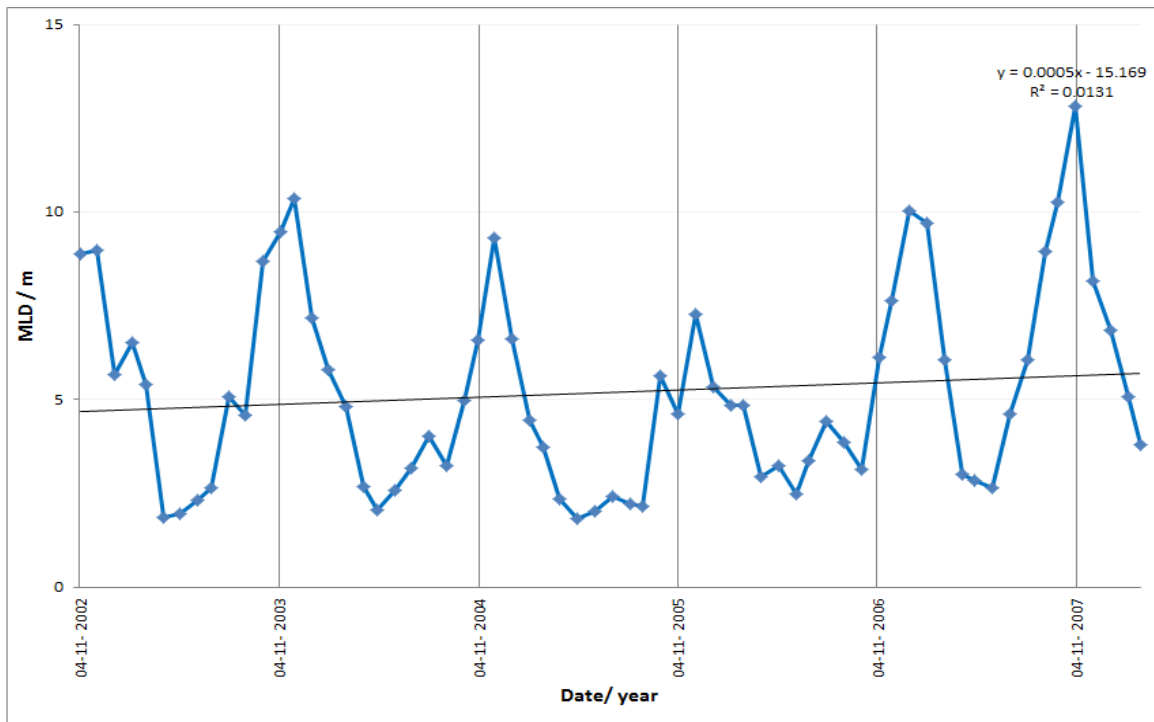


Figure 4.19: Monthly data of mixed layer depth (MLD) for the years from 2003 until 2007 to the South zone of the Red Sea. The monthly south look smooth as the middle

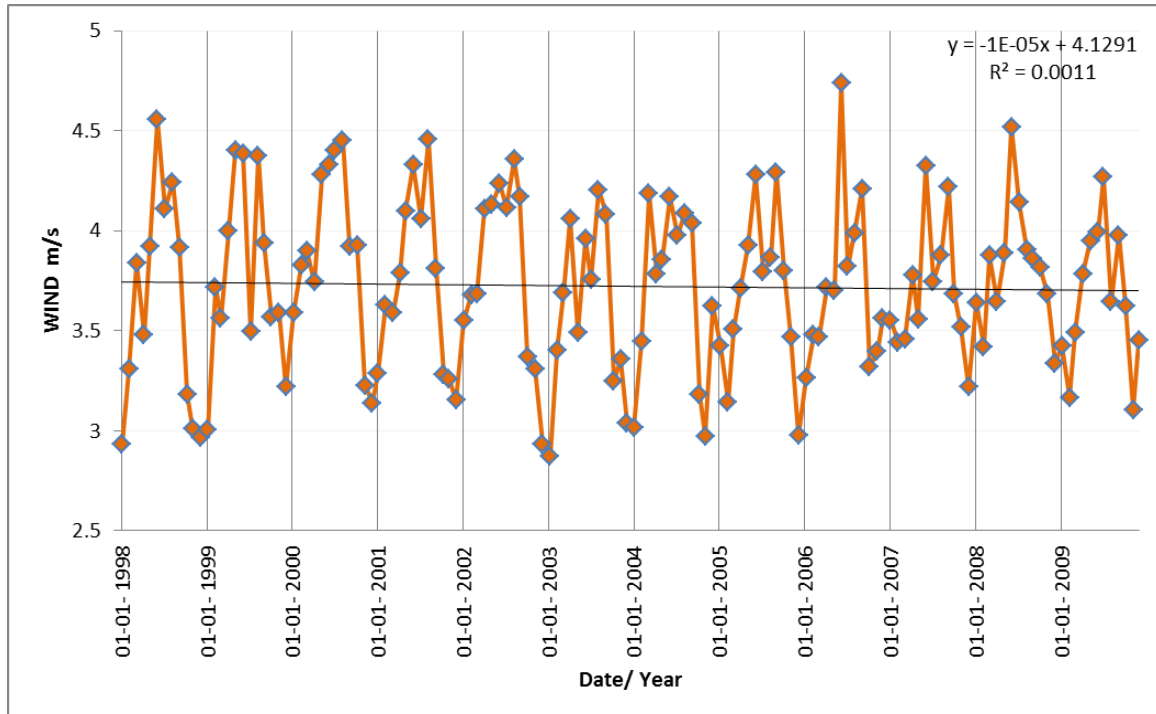


Figure 4.20: Monthly data of WIND for the period from 1998 until 2009 in the Middle zone of the Red Sea.

Table 4.5: Monthly correlations of CHL with other parameters South Zone of the Red Sea.

correlation	SST	PAR	MLD	Wind
CHL-a	-0.292	-0.610	-0.5294	0.740

Interannulay, the anomalies variation in this zone is weaker than the other zones. The CHL-a varies from -0.003 to 0.021. But the last value is the same -0.003. In the mixed layer plot, the limited years shows that the variation is not like CHL-a. It is in the positive side in the plot (see Figure 4.21 and Table 4.6).

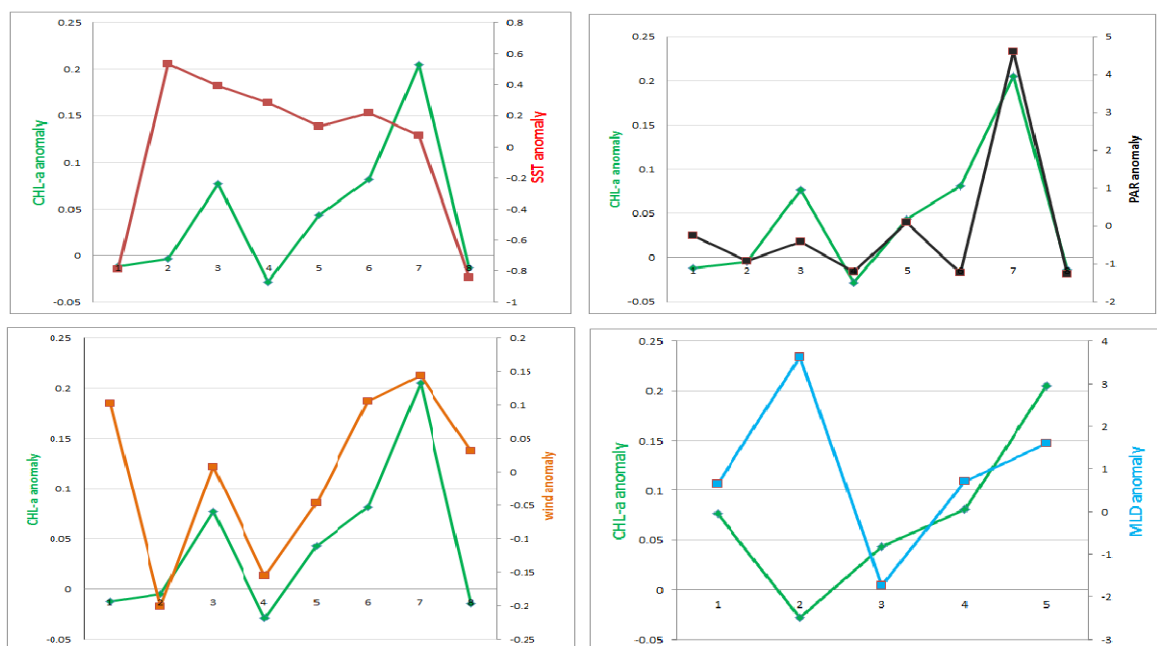


Figure 4.21: plot of Anomalies of CHL-a with other parameters in South zone of Red Sea. For each parameter, each monthly value was subtracted from monthly climatology

Table 4.6: Anomalies correlation of CHL with other parameters South Zone of Red Sea

corrlation	SST	PAR	MLD	Wind
CHL-a	0.277	0.845	-0.0166	0.598

What we expected in the southern zone of the Red sea is as follows: the chlorophyll-a dynamics should be controlled by wind.

This zone shows that the blooms starts during the summer(September), this is not as usual and that is because: this zone of the Red Sea is near the Arabian Sea which has a high value of the chlorophyll during the bloom. Water goes from The Arabian Sea to the south of the Red Sea during winter, the south-west during winter pushes the water from Arabian Sea into the Red Sea, and the nutrients are carried by water, which is important for the photosynthesis proceses.

Monthly plots and correlation showed that the blooms in this zone are controlled by MLD, even though the possotive correlation between MLD and CHL-a in monthly data in the south zone, we cannot prove that the MLd controlled the bloom because it was few meters approximately(10m), where the nutrients are deeper than that. The anomalies plots and correlation showed different results as the blooms here are controlled by two parameters, PAR and wind. I would rather state that the wind is the main factor which controlled the chlorophyll-a blooms in this zone, because in all of the Red Sea area, PAR is there throughout the year, even with the strong correlation (0.845) which PAR shows. Nevertheless, I maintain that the wind controlled the blooms in this zone of the Red Sea.

During the years which show different peaks than other years (1999, 2008 and 2009), there are no special variations of the physical parameters during these years, which show that these high or even low values are in accordance to the specific parameter.

Chapter 5

Conclusion and Recommendation

Interannually, the control of physical parameters is different between monthly and anomalies data. For example, in the north zone of the Red Sea the monthly correlation is (-0.429), while the anomaly correlation is (0.722) in the same zone. The correlation is changed totally from negative to positive.

the first three years in the north zone had low values of CHL-a. The trend line increases from 1998 until 2009. This was shown clearly from the variation of anomalies from (-0.0035 to 0.028). And that due to the high values in the last two years.

In the middle, the CHL-a anomalies had less variation than the north zone. It vary from (-0.015 to -0.035). The highest values during whole years appeared clearly with the high variation which showed on the anomalies plot.

The south zone had a weak variation at all. Because the all years had close to each other, so the variation had a lower range between (-0.003 to 0.021). The last three years had high values of CHL-a and wind. That proved the south zone in controlled by wind which the correlation showed 0.7408 and 0.598 in the monthly and anomaly data, respectively.

Finally, I recommend to have nutrients data. With these physical parameters which are always have low quality; we cannot prove exactly what control the blooms in the three zones. During the blooms, some substances which are important for photosynthesis such as Nitrate and Iron are consumed by phytoplankton, by measuring these substances in the three zones, we will know exactly the time and the mangnitude of the blooms in the Red Sea.

Bibliography

- Acker, J., Leptoukh, G., Shen, S., Zhu, T., and Kempler, S. (2008). Remotely-sensed chlorophyll a observations of the northern Red Sea indicate seasonal variability and influence of coastal reefs. *Journal of marine systems*, **69**(3):pp. 191–204.
- Aiken, J., Moore, G.F., and Hotligan, P.M. (1992). Remote sensing of oceanic biology in relation to global climate change. *Journal of phycology*, **28**(5):pp. 579–590.
- Ali, Elsheikh Bashir (2008). *The inorganic carbon cycle in the Red Sea*. Master's thesis, university of bergen.
- Barker, H.A. (1935). Photosynthesis in diatoms. *Archives of Microbiology*, **6**(1):pp. 141–156.
- Brock, J.C. and McClain, C.R. (1992). Interannual variability in phytoplankton blooms observed in the northwestern Arabian Sea during the southwest monsoon. *Journal of Geophysical Research*, **97**(C1):pp. 733–750.
- Butler, MJA (1988). *The application of remote sensing technology to marine fisheries: an introductory manual*. 295-297. Food and Agriculture Organization of the United Nations.
- Chisholm, S.W. and Morel, F.M.M. (1991). What controls phytoplankton production in nutrient-rich areas of the open sea. *Limnol. Oceanogr*, **36**(8):pp. 1507–1965.
- de Boyer Montégut, C., Madec, G., Fischer, A.S., Lazar, A., and Iudicone, D. (2004). Mixed layer depth over the global ocean: An examination of profile data and a profile-based climatology. *J. Geophys. Res*, **109**(C12):page C12,003.
- Dowidar, N.M. (1974). the phytoplankton of the Mediterranean waters of Egypt. I. A check list of the species recorded. *Egyptian Bulletin of National Institute of Oceanography & Fisheries, ARE*, **4**:pp. 319–344.

Bibliography

- Edwards, F.J. (1987). Climate and oceanography. *Red Sea, Pergamon Press, Oxford*:pp. 45–69.
- Eppley, R.W., Renger, E.H., Venrick, E.L., and Mullin, M.M. (1973). A study of plankton dynamics and nutrient cycling in the central gyre of the North Pacific Ocean. *Limnol. Oceanogr*, **18**(4):pp. 534–551.
- Evans, R.H. and Gordon, H.R. (1994). Coastal zone color scanner" system calibration": A retrospective examination. *JOURNAL OF GEOPHYSICAL RESEARCH-ALL SERIES-*, **99**:pp. 7293–7293.
- Fahmy, M. (2003). Water quality in the Red Sea coastal waters (Egypt): Analysis of spatial and temporal variability. *Chemistry and Ecology*, **19**(1):pp. 67–77.
- Frouin, R., Franz, B., and Wang, M. (2001). Algorithm to estimate PAR from SeaWiFS data Version 1.2-Documentation. *Ocean Colour Products*.
- Frouin, R., Lingner, D.W., and Gautier, C. (1989). A Simple Analytical Formula to Compute Clear Sky Total and Photosynthetically Available Solar Irradiance. *Journal of Geophysical Research*, **94**(C7):pp. 9731–9742.
- Gill, A.E. (1982). *Atmosphere-ocean dynamics*, volume 30. Academic Pr.
- Halim, Y. (1969). Plankton of the Red Sea. *Oceanography and Marine Biology: an annual review*, **7**.
- Hooker, S., Firestone, E., Esaias, W., Feildman, G., Gregg, W., and McClain, C. (1992). SeaWiFS technical report series. Volume 1: An overview of SeaWiFS and ocean color.
- Hovis, W.A., Clark, D.K., Anderson, F., Austin, R.W., Wilson, W.H., Baker, E.T., Ball, D., Gordon, H.R., Mueller, J.L., El-Sayed, S.Z., et al. (1980). Nimbus-7 Coastal Zone Color Scanner: system description and initial imagery. *Science*, **210**(4465):page 60.
- Jeffrey, SW, Mantoura, RFC, et al. (1997). Development of pigment methods for oceanography: SCOR-supported working groups and objectives. *Monographs on Oceanographic Methodology*, **10**.

- Kneubuehler, M., Schaepman, M.E., Thome, K.J., and Schlapfer, D.R. (2003). MERIS/ENVISAT vicarious calibration over land. In: *Proceedings of SPIE*. volume 5234, (pp. 614–623).
- Kotb, M., Abdulaziz, M., Al-Agwan, Z., Alshaikh, K., Al-Yami, H., Banajah, A., Devantier, L., Eisinger, M., Eltayeb, M., Hassan, M., et al. (2004). Status of coral reefs in the Red Sea and Gulf of Aden in 2004.
- Labiosa, R.G., Arrigo, K.R., Genin, A., Monismith, S.G., and van Dijken, G. (2003). The interplay between upwelling and deep convective mixing in determining the seasonal phytoplankton dynamics in the Gulf of Aqaba: Evidence from SeaWiFS and MODIS. *Limnology and oceanography*:pp. 2355–2368.
- Levanon-Spanier, I., Padan, E., and Reiss, Z. (1979). Primary production in a desert-enclosed sea-the Gulf of Elat (Aqaba), Red Sea. *Deep Sea Research Part A. Oceanographic Research Papers*, **26**(6):pp. 673–685.
- Mann, K.H. and Lazier, J.R.N. (2006). *Dynamics of marine ecosystems: biological-physical interactions in the oceans*. Wiley-Blackwell.
- Martin, S. (2004). *An introduction to ocean remote sensing*. Cambridge University Press.
- Minnett, P.J., Smith, M., and Ward, B. (2011). Measurements of the oceanic thermal skin effect. *Deep Sea Research Part II: Topical Studies in Oceanography*, **58**(6):pp. 861–868.
- Mishke, O.K., Volkovinsky, V.V., and Kabanova, J.G. (1970). *Plankton primary production of the world ocean*.
- Moore, J.K., Doney, S.C., Glover, D.M., and Fung, I.Y. (2001). Iron cycling and nutrient-limitation patterns in surface waters of the World Ocean. *Deep Sea Research Part II: Topical Studies in Oceanography*, **49**(1-3):pp. 463–507.
- Morel, A. and André, J.M. (1991). Pigment distribution and primary production in the western Mediterranean as derived and modeled from Coastal Zone Color Scanner observations. *Journal of Geophysical Research*, **96**(C7):pp. 12,685–12.
- NASA (2012a). about MODIS. <http://modis.gsfc.nasa.gov/about/>.

Bibliography

- NASA (2012b). Background of the SeaWiFS Project. http://oceancolor.gsfc.nasa.gov/SeaWiFS/BACKGROUND/SEAWIFS_BACKGROUND.html.
- Nielsen, E.S. (1978). Growth of plankton algae as a function of n-concentration, measured by means of batch technique. *Marine Biology*, **46**(3):pp. 185–189.
- Patzert, W.C. (1974). Wind-induced reversal in Red Sea circulation. In: *Deep Sea Research and Oceanographic Abstracts*. Elsevier, volume 21, (pp. 109–121).
- Pratt, L.J., Deese, H.E., Murray, S.P., and Johns, W. (2000). Continuous Dynamical Modes in Straits Having Arbitrary Cross Sections, with Applications to the Bab al Mandab. *Journal of physical oceanography*, **30**(10):pp. 2515–2534.
- Pratt, L.J., Johns, W., Murray, S.P., and Katsumata, K. (1999). Hydraulic Interpretation of Direct Velocity Measurements in the Bab al Mandab. *Journal of physical oceanography*, **29**(11):pp. 2769–2784.
- Robinson, I.S. (2010). *Discovering the Ocean from Space: The unique applications of satellite oceanography*. Springer.
- Sarma (2012). Inter-annual Variability of Chlorophyll-a in the Arabian Sea and its Gulfs. *Technical Report 1*, International Journal of Marine Science.
- Sathyendranath, S. et al. (2000). Remote Sensing of Ocean Colour in Coastal, and Other Optically-Complex, Waters, reports of the International Ocean-Colour Coordination Group, no. 3. *Reports and Monographs of the International Ocean-Colour Coordinating Group (IOCCG)*, **3**.
- Shaikh, E.A., Roff, J.C., and Dowidar, N.M. (1986). Phytoplankton ecology and production in the Red Sea off Jiddah, Saudi Arabia. *Marine Biology*, **92**(3):pp. 405–416.
- Siegel, D.A., Doney, S.C., and Yoder, J.A. (2002). The North Atlantic spring phytoplankton bloom and Sverdrup's critical depth hypothesis. *Science*, **296**(5568):pp. 730–733.
- Smeed, D. (1997). Seasonal variation of the flow in the strait of Bab al Mandab. *Oceanologica acta*, **20**(6):pp. 773–781.

- Smeed, D.A. (2000). Hydraulic control of three-layer exchange flows: Application to the Bab al Mandab. *Journal of Physical Oceanography*, **30**(10):pp. 2574–2588.
- Smeed, D.A. (2004). Exchange through the Bab el Mandab. *Deep Sea Research Part II: Topical Studies in Oceanography*, **51**(4):pp. 455–474.
- Sofianos, S.S. and Johns, W.E. (2002). An Oceanic General Circulation Model (OGCM) investigation of the Red Sea circulation, 1. Exchange between the Red Sea and the Indian Ocean. *Journal of geophysical research*, **107**(C11):page 3196.
- Sofianos, S.S. and Johns, W.E. (2003). An oceanic general circulation model (OGCM) investigation of the Red Sea circulation: 2. Three-dimensional circulation in the Red Sea. *J. Geophys. Res*, **108**:page 3066.
- Susanto, R. and Marra, J. (2005). Chlorophyll a Variability. *Oceanography*, **18**(4):page 124.
- Weikert, H. (1987). Plankton and the pelagic environment. *Red Sea, Pergamon Press, Oxford*:pp. 90–111.
- Wikipedia (2012). Red Sea. http://en.wikipedia.org/wiki/Red_Sea.
- Yentsch, C.S. (1960). The influence of phytoplankton pigments on the colour of sea water. *Deep Sea Research (1953)*, **7**(1):pp. 1–9.

